nature biomedical engineering

REVIEW ARTICLE

PUBLISHED: 10 JANUARY 2017 | VOLUME: 1 | ARTICLE NUMBER: 0008

Light in diagnosis, therapy and surgery

Seok Hyun Yun[1,2,3]* and Sheldon J. J. Kwok[1,3]

Light and optical techniques have made profound impacts on modern medicine, with numerous lasers and optical devices currently being used in clinical practice to assess health and treat disease. Recent advances in biomedical optics have enabled increasingly sophisticated technologies — in particular, those that integrate photonics with nanotechnology, biomaterials and genetic engineering. In this Review, we revisit the fundamentals of light–matter interactions, describe the applications of light in imaging, diagnosis, therapy and surgery, overview their clinical use, and discuss the promise of emerging light-based technologies.

The modern use of light in medicine began in the nineteenth century, with rapid improvements in the understanding of both the physical nature of light and fundamental light–matter interactions. A notable example of an early triumph in phototherapy is the ultraviolet (UV)-induced treatment of lupus vulgaris invented by physician Niels Finsen, who in 1903 was awarded the Nobel Prize in Physiology and Medicine for this application. Since 1960, the development of lasers has opened new medical avenues. Today, numerous laser-based therapeutic and diagnostic devices are routinely used in the clinic.

Within tissue, photons interact with biological matter via various processes, which can be broadly categorized into scattering and absorption (Fig. 1a and Box 1). Scattering can alter the propagation path, polarization and spectrum of incident light. The states of the scattered light can be analysed and mapped for diagnosis and imaging. In light absorption, the energy of photons is converted to electronic or vibrational energy in the absorbing molecule. Some of that energy can be re-emitted through luminescence (for example, fluorescence), inelastic scattering, or acoustomechanical waves. Such emission from the tissue carries information about its microstructure and molecular contents, and serves as the basis for optical diagnostics and imaging. On the other hand, photoexcitation of intrinsic molecules or exogenous light-sensitive agents introduced in the body can affect the tissues and cells within in various ways, via the generation of heat (photothermal), chemical reactions (photochemical) and biological processes (photobiological or optogenetic). Optical therapy and laser surgery use these effects in a controlled manner.

X-rays and gamma rays have transformed modern medicine by enabling computed tomography (CT) and positron emission tomography (PET), as well as radiation therapy. Radio waves and magnetic fields have made magnetic resonance imaging (MRI) possible. Among the wide spectrum of electromagnetic waves, light comprises a region from the deep blue to the near-infrared (NIR) and provides a distinct advantage due to its unique photon energy range of 0.5–3 eV. These energies fall into a window that permits rich yet safe interactions with organic molecules. At higher energies, bond dissociation (>3.6 eV for C–C and C–H bonds) and ionization (>7 eV) can occur; and at lower energies, water absorption dominates, preventing any specific targeting of molecules. Light-based technologies in medicine take advantage of the variety of light–molecule interactions in this optical window (Box 2).

In what follows, we overview the major applications of light in three categories: optical diagnosis, laser surgery and light-activated therapy (Fig. 2a). We also discuss optical imaging, which plays important roles in diagnosis, surgical guidance and therapy monitoring. For each technology, we briefly highlight its principle of operation, advantages and limitations, and current clinical utilities. We then describe emerging light-based technologies, with particular emphasis on opportunities in nanomedicine, optogenetics and implantable devices.

Laser surgery

The development of lasers expanded the therapeutic applications of light well beyond the long-known effects of sunlight and focused lamps. With lasers, emission intensities can be several orders of magnitude higher than that of sunlight, short pulses are readily generated and wavelengths can be precisely selected. Physicians started exploring the medical applications of lasers after the first demonstration of the ruby laser by Maiman in 1960, when biohazards of high-intensity laser pulses to the eye and skin became appreciated. Photocoagulation in the retina[1], destruction of skin lesions[2] and removal of dental caries and cardiovascular plaques are examples of early pioneering works. Today, medical lasers are routinely used in many applications, including surgeries in ophthalmology, the treatment of cutaneous disorders, and tissue ablation in internal organs through fibre-optic delivery. This has led to a global market for therapeutic lasers estimated to be over US$3 billion (Fig. 2b,c).

Laser surgery in ophthalmology. The ablative ability of UV photons from an ArF excimer laser (193 nm) to reshape the cornea is widely used for refractive error correction[3]. UV radiation breaks the peptide bonds of collagen fibres within the cornea, expelling a discrete volume of corneal tissue from the surface[4] (Fig. 3a). For example, a single excimer pulse (0.25 J cm^{-2}) with a spot size of 1 mm removes about 0.25 μm of tissue. A customized scanning pattern generated by optical wavefront analysis of the patient is used to precisely reshape the patient's cornea. Unlike photorefractive keratectomy, where the corneal epithelium is irradiated, laser-assisted *in situ* keratomileusis (LASIK) ablates corneal stroma through an ~160-μm-thick corneal flap that is prepared by using femtosecond Nd:glass laser pulses (600 fs; 1,053 nm) focused to a spot size of 2–3 μm. Millions of LASIK procedures have been performed in the past two decades, with a 95.4% overall patient satisfaction in a recent meta-analysis[5]. Laser thermal keratoplasty uses holmium:YAG (2,100 nm) laser energy to reshape the cornea but is less used due to plastic regression after treatment.

[1]Wellman Center for Photomedicine, Massachusetts General Hospital, 65 Landsdowne Street, Cambridge, Massachusetts 02139, USA. [2]Department of Dermatology, Harvard Medical School, 25 Shattuck Street, Boston, Massachusetts 02115, USA. [3]Harvard–MIT Health Sciences and Technology, 77 Massachusetts Avenue, Cambridge, Massachusetts 02139, USA. *e-mail: syun@hms.harvard.edu

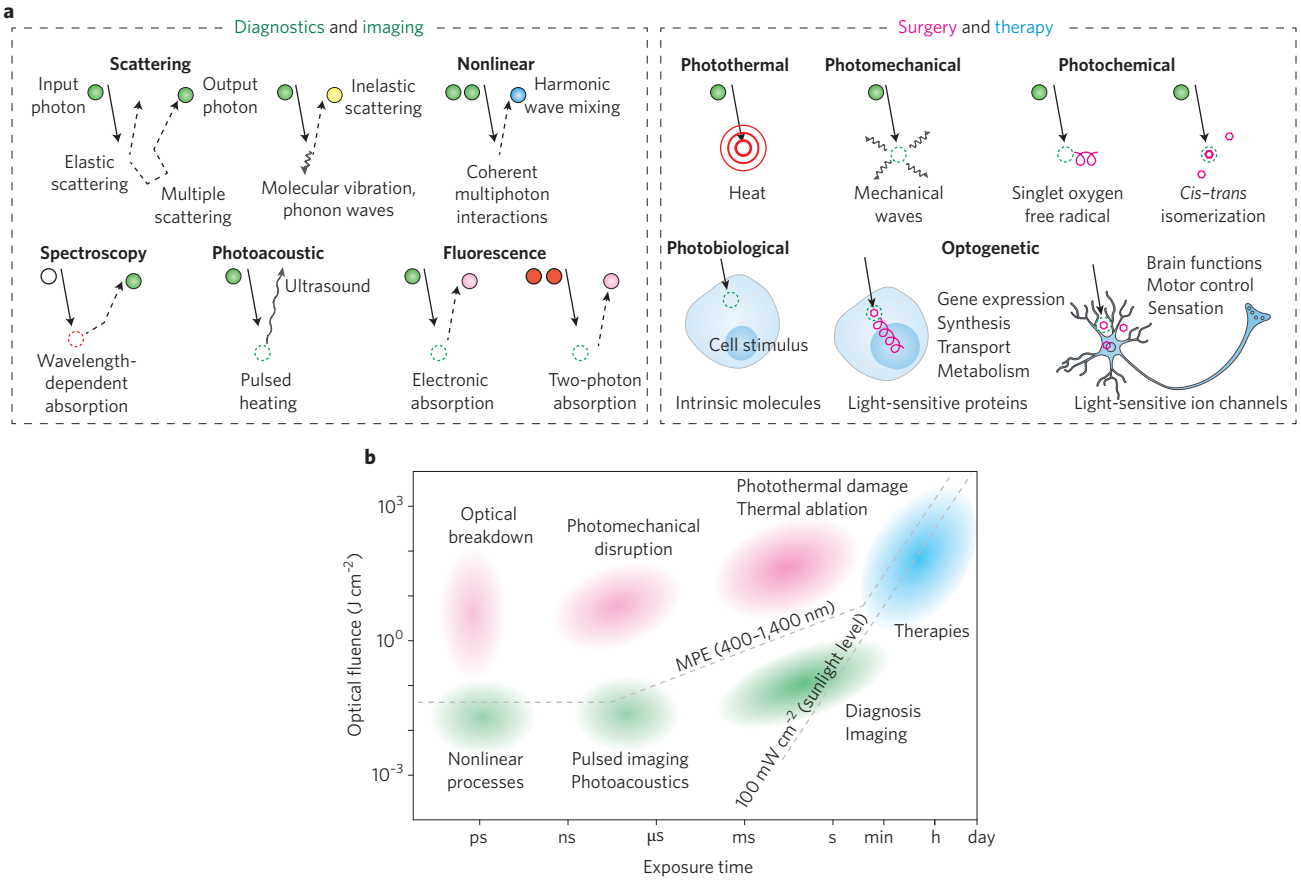

Figure 1 | Light–tissue interactions. a, Representative optical mechanisms used in diagnosis and imaging (left), and surgery and therapy (right). Circular objects denote incoming and outgoing photons, with their trajectories indicated by solid and dotted arrows. Colours of the circles represent the spectrum of the light; dotted circles indicate the absorption of input photons. For the case of therapy, specific effects of light on tissue and cells are indicated. **b**, Optical techniques mapped according to their optical fluence and exposure time (either total illumination time for continuous-wave light, or pulse duration for pulses). Colours represent medical areas: green for diagnostics, pink for surgery and blue for therapy. MPE, maximum permissible exposure.

A cataract in the lens is the leading cause of preventable blindness worldwide; in fact, over 20 million cataract surgeries are performed annually. In these, a laser is used to create an incision on the lens capsule and gain access to the cataract. Nd:YAG laser capsulotomy is used to treat posterior capsule opacification, which occurs in about 20% of patients following cataract surgery. Although the disruption of the crystalline lens is done by ultrasound, femtosecond laser technology for cataract surgery may offer a more reliable and improved safety profile[6].

Laser coagulation therapy is a common procedure to seal a retinal tear or small retinal detachment[7] (Fig. 3b), shrink abnormal blood vessels in proliferative diabetic retinopathy and seal blood vessels in retinal edema[8]. Green and yellow wavelengths, well absorbed by oxyhaemoglobin and melanin, are suitable for photocoagulation. Typically, this procedure uses a potassium titanyl phosphate (KTP)-based frequency-doubled Nd:YAG laser (532 nm), krypton ion laser (531 or 568 nm), or a diode-pumped dye laser (577 nm) at a typical fluence of 100 J cm^{-2} and duration of 10–100 ms per pulse.

Dermatological and aesthetic treatments. Since the laser was invented, efforts have been made to develop more effective lasers for the removal of unwanted skin markings, including tattoos, birth marks, stretch marks, port-wine stains, acne scars and leg veins[9]. Cutaneous laser surgery was revolutionized by the concept of selective photothermolysis[10], which states that optical pulses with optimal parameters — wavelength, duration, beam size and energy — can selectively destruct a target within the skin, minimizing the risk of scarring and damage to normal tissue. A pulsed dye laser (PDL) tuned at 585 nm (0.4–2 ms; 5–10 J cm^{-2}) removes skin markings by selectively targeting haemoglobin within red blood cells, with minimal thermal damage to other structures[11]. Spot sizes of 2–10 mm are used to permit deeper dermal penetration and the destruction of larger blood vessels. A PDL is useful in the treatment of port-wine stains, superficial haemangiomas and other vascular lesions. A cryogen-cooling device is used to limit the temperature rise at the surface of the skin while allowing heat accumulation at the target region underneath[12]. A PDL is also used to treat non-vascular lesions such as hypertrophic scars, keloids and striae.

Laser skin resurfacing can reduce facial wrinkles, scars and pimples. Indeed, ablative therapy using CO_2 lasers (10.6 µm; 1–10 ns; 5 J cm^{-2}) is the current gold standard[13]. However, the Er:YAG laser (2,940 nm) has a higher water absorption (12,800 cm^{-1}) than the CO_2 laser (800 cm^{-1}), ablating 5–20 µm of tissue at 5 J cm^{-2}. Alternatively, non-ablative resurfacing can minimize risk and shorten recovery times by producing dermal thermal injury to reduce rhytides (skin wrinkles) and photodamage while preserving the epidermis. Moreover, fractional resurfacing thermally coagulates or ablates microscopic columns of epidermal and dermal tissue in a regularly spaced array that is followed by rapid re-epithelization and dermal remodelling, which reduces the risk of scarring, improves treatment efficacy and shortens recovery time[14]. Fractionated lasers are divided into non-ablative NIR lasers (typically 1,550 nm)[15] and ablative infrared lasers (typically 10.6 µm)[16] (Fig. 3c).

When targeting melanin, laser treatment can lighten or remove benign epidermal and dermal pigmented lesions as well as tattoos. To induce rapid ablative heating, nanosecond Q-switched pulses

Box 1 | Light–tissue interactions.

Different diagnostic and therapeutic applications of light require a specific optimal choice of optical parameters, including wavelength λ, exposure time τ, beam area A, energy E, power $P = E/\tau$, intensity P/A and fluence E/A (Fig. 1b).

Light scattering. Elastic light scattering occurs due to inhomogeneous electric polarization density in tissues. The magnitude of Rayleigh scattering from atoms and molecules is proportional to $1/\lambda^4$, and Mie-type scattering due to microscopic index variations is nearly independent of λ. The experimentally measured 'reduced' scattering coefficients fit well with $a \times \lambda^{-b}$, where b ranges from 0.7 to 1.6 and a varies from 19 to 79 cm^{-1}, depending on tissue type[235]. Inelastic light scattering arises from moving scatterers (dynamic light scattering), thermodynamically produced hypersonic waves (Brillouin scattering) and molecular vibrations (Raman scattering). The scattering coefficients for spontaneous inelastic scattering are several orders of magnitude lower than those for elastic scattering.

Penetration depths. Scattering and absorption limit how far light can diffuse into tissue. In skin tissues, the effective penetration depth at which the incident optical energy drops to $1/e$ (~37%) is typically 50–100 μm for UV and blue light (λ = 400–450 nm) and also for infrared light above 2,000 nm because of high light absorption by water. The penetration depth of green light (500–550 nm) is a few hundreds of micrometres, limited by light absorption by melanin and haemoglobin. The penetration depth is the largest, typically 1–3 mm, for red and NIR light (600–1,350 nm).

Photothermal effects. The local temperature of tissues increases as a result of laser absorption. Hyperthermia occurs near 42.5–43.0 °C, tissue coagulation and welding occurs typically at 60–70 °C, and higher temperatures lead to tissue ablation via vaporization (100 °C) and carbonization (300–450 °C). The required energy depends on the desired temperature, light penetration, and target tissue volume. Without heat dissipation, it takes approximately 4 J (heat capacity) to increase the temperature of 1 cm^3 of tissue by 1 °C and ~2.7 kJ (latent heat of water) to vaporize the water in the tissue. For example, when a laser beam with a short penetration depth of 100 μm is illuminated over an area of 1 cm^2, a fluence of 1 J cm^{-2} will raise the temperature of the tissue surface by 25 °C above body temperature (62 °C), at which protein denaturation occurs. A fluence of 25 J cm^{-2} would heat and vaporize the 100-μm-thick layer of tissue to 100 °C and thereby ablate it.

Pulsed irradiation is commonly used to avoid heat diffusion during irradiation and to minimize collateral tissue damage. For ablation of large tissue volumes, pulse widths of 1–100 ms are adequate; for high-precision ablation, micro- and nanosecond pulses are needed. The thermal diffusion length, $(4\alpha\tau)^{1/2}$, where α = ~1.4×10^{-7} cm^2 s^{-1} is the heat diffusivity in tissue, is 1.2 mm for continuous-wave illumination for τ = 10 s, yet only 37 nm for short pulses with τ = 10 ns. The peak temperature at which irreversible tissue damage occurs depends on exposure time: according to the Arrhenius model[236], protein denaturation is induced at 60 °C for τ = 1 s but requires 90 °C for τ = 10 ns.

Photomechanical effects. In tissue, localized absorption of short laser pulses (<1 μs) leads to a local rise in pressure (~800 kPa per degree Celsius), which generates propagating stress waves with acoustic energy increasing with the square of optical pulse energy. For diagnosis, low optical intensity is used, which limits the temperature rise to less than 1 °C, and generated ultrasound waves are detected for mapping the concentration of light-absorbing molecules. At high optical intensity, shock waves can cause mechanical disruption, often of enough intensity to fragment kidney stones. Photoablation by a pulsed excimer (or exciplex) laser involves molecular bond breakage by intense UV light, followed by mechanical ejection of the tissue[237]. And femtosecond mode-locked laser pulses (~100 fs) focused to a small spot size at high intensity can generate plasma (that is, ionized gas) at extremely high temperature — a process known as optical breakdown — that can ablate tissue and make a clean cut with negligible collateral thermal damage through complex processes involving mechanical ejection of tissue.

Photochemical and photobiological effects. Upon absorbing a photon, an excited molecule can interact with a neighbouring molecule to cause photochemical effects, such as the generation of free radicals and singlet oxygen, as well as photobiological effects, such as the destruction of enzymes in cellular signalling pathways, the opening of ion channels, and the promotion of specific gene expression. Although this process involves one photon per molecule, a large number of incident photons are needed: the number is approximately equal to A/σ_a, where σ_a is the molecule's absorption cross-section (which is easily determined from a molar extinction measurement). Most light-absorbing organic molecules have peak extinction coefficients of 10^4–10^5 M^{-1} cm^{-1}. For example, the peak extinction coefficient for human rhodopsin is 40,000 M^{-1} cm^{-1} at 493 nm, and therefore $\sigma_a = 2 \times 10^{-16}$ cm^2. The average optical fluence required to excite one rhodopsin molecule (at 63% probability) is E_p/σ_a = 2 mJ cm^{-2}, where E_p is the photon energy. Although optical fluence on the order of 1–10 mJ cm^{-2} is sufficient for photoexcitation *in vitro*, in tissue a higher optical energy is necessary to compensate for optical loss. Furthermore, the typical efficiency (quantum yield) of a photochemical reaction ranges from 10% to 80%, and a molecule may be excited multiple times to enhance the photochemical effect. For this reason, the optimal dose required in medical applications often exceeds 1 J cm^{-2}. At this level, photothermal tissue damage is minimal (<2.5 °C) when visible or NIR light with a penetration depth longer than 1 mm is used.

Safety limits for diagnosis and imaging. Diagnostic applications demand low optical powers for safety. For optical radiation, the requirement is quantified in terms of the maximum permissible exposure (MPE), which is defined as one tenth of the damage threshold resulting from photothermal and photochemical effects. According to the standard guideline[238], laser-exposure limits for the skin are given as $0.02C_A$ J cm^{-2} for τ = 1–100 ns, and $1.1C_A\tau^{0.25}$ J cm^{-2} for τ = 100 ns to τ = 10 s (where the empirical coefficient C_A is 1 for λ = 400–700 nm and increases to 5 for λ = 1,050–1,400 nm). For exposures of $\tau > 10$ s, the MPE is $2C_A$ W cm^{-2} (in this case, the MPE is given in intensity units because thermal equilibrium is reached between laser-induced heating and conductive cooling).

(10–100 ns; 3–7 J cm^{-2}; 1–10 Hz) are the usual choice. The optimal laser wavelength depends on specific skin types, target depth and pigment absorption. Q-switched ruby (694 nm), alexandrite (755 nm) and Nd:YAG (1,064 nm) lasers are typically used[17]. Superficial lesions are treated with shorter wavelengths (510 nm for PDL; 532 nm for KTP). Also, a picosecond alexandrite laser has been developed for targeting smaller pigments[18].

Laser hair removal uses light pulses targeting melanin in the hair shaft and hair follicle to achieve long-lasting removal of excessive hairs in cosmetically undesirable locations[19]. Because of the

Box 2 | Why light for medicine?

Plants have sophisticated energy-harvesting machinery to convert solar energy, highest in the 400–700 nm spectral range[239], into chemical energy. Microorganisms, such as green algae, have light-gated ion channels that enable phototaxis and thus enhanced energy harvest. The vision system of higher organisms is based on phototransduction proteins, which help the organisms search for food and keep away from danger. Fruit flies and jellyfish generate bioluminescence, and insects and birds reflect colourful irradiance with photonic crystal structures for improved survival and reproduction. These examples illustrate not only the extraordinary connection between light and biology, but also the role of light as an important determinant and driving force of natural evolution.

The use of light in medicine is an extension of the evolutionary role of light in biology. Colour perception is mediated by the absorption of light by three types of cone cell in the eye (blue, green and red, with respective wavelengths of 400–450 nm, 500–570 nm and 610–750 nm). Yet various types of light–tissue interaction generate contrast beyond what can be perceived by the naked eye, enabling molecular imaging of cells and tissues at high resolutions. The therapeutic effects of light on tissues can be traced to the absorption of specific wavelengths by a variety of light-sensitive molecules that are endogenously present in the human body or may be inserted via gene-editing technologies. Most likely, medicine will benefit from increasingly sophisticated light-based technologies that use materials and machineries resulting from billions of years of evolution.

presence of melanin in the epidermis, active cooling of the skin by spray or contact cooling is critical to minimize unwanted thermal injury of the tissue. A variety of lasers emitting long pulses (1–600 ms; 10–50 J cm^{-2}), such as the ruby laser, the alexandrite laser, semiconductor diode lasers (800–810 nm) and flash lamp-based intense pulsed light (IPL) sources (550–1,200 nm) are suited for photoepilation.

Recently, a number of hand-held light sources have become available as consumer cosmetic products for home use in applications including photorejuvenation, hair growth, hair removal and acne treatment[20]. Advances in compact fibre lasers in the NIR range may also replace some of the existing solid-state Nd:YAG and holmium:YAG lasers used in the clinic[21].

Laser surgery in urology and gastroenterology. Benign prostate hyperplasia is a non-cancerous condition affecting about 50% of men by the age of 50 and up to 90% older than 80, in which an enlarged prostate squeezes or partially blocks the surrounding urethra. A high-power laser (80–180 W; 20 ms; 400 J cm^{-2}) is used to remove the excess tissue. Holmium-laser enucleation or ablation of the prostate[22], developed in the 1990s, is less popular compared with transurethral resection using electrical loops. A rapidly growing laser-surgery technique for the prostate is photoselective vaporization using a frequency-doubled Nd:YAG laser (532 nm) delivered fibre-optically through a cystoscope[23] (Fig. 3d). Medicare estimated that ~72,000 photoselective vaporization procedures were performed in the United States in 2008 (accounting for 27% of all benign prostate-hyperplasia surgeries), whereas transurethral resection amounted to 64% of surgeries.

Lithotripsy is a surgical procedure to remove stones from the urinary tract (kidney, ureter, bladder or urethra) in patients with urinary calculi (stones). When ultrasound-based shock-wave lithotripsy cannot be used, lithotripsy is performed using a holmium:YAG laser through a flexible ureteroscope[24]. Laser lithotripsy is also used for the fragmentation of intraductal gallstones, particularly stones that cannot be targeted by conventional mechanical lithotripsy[25].

Lasers in cardiology and vascular surgery. Laser-assisted lead extraction is a highly effective procedure for the extraction of lead wires of cardiac pacemakers and defibrillators from coronary blood vessels[26]. This method uses a special sheath that conducts laser pulses to the distal tip as a ring of light to break up scar tissue around the lead, facilitating removal. Typically, XeCl laser pulses (100–200 ns; 3–6 J cm^{-2}) are used, causing localized ablation of the ~100 μm of tissue in front of the tip[27].

An early approach for angioplasty in the treatment of coronary artery disease was excimer laser ablation of plaques through a fibre-optic catheter[28]. However, its use has declined in recent years. Endovenous laser treatment is effective for treating lower-extremity venous insufficiency such as great saphenous vein reflux[29]. High-power laser light, typically from continuous-wave NIR diode lasers (810, 940 or 1,470 nm; 10–30 W), is intravenously delivered through a fibre-optic catheter to ablate varicose veins[30]. For asymptomatic lower-extremity telangiectasias, lasers (Nd:YAG, diode, KTP) are applied externally, particularly when sclerotherapy is not feasible[31].

Other applications. Various dental lasers have been used to remove and modify soft and hard tissues in the oral cavity. For instance, CO_2, Nd:YAG and diode lasers are used for soft-tissue removal such as in gingivectomy, for killing bacteria and for promoting the regrowth of tissues. Applications to hard tissue (enamel and dentin), such as dental drilling using highly ablative Er:YAG lasers[32], are also growing[33].

In otolaryngology, the CO_2 laser is routinely used because of its minimal lateral tissue damage particularly in larynx surgery[34]. Interstitial laser coagulation has shown potential for causing necrosis of small tumour metastases[35]. Endoscopic laser therapy can be used for the palliation of advanced esophageal cancers[36]. And Nd:YAG lasers are used in bronchoscopic laser resection to relieve intraluminal airway obstruction caused by bronchogenic carcinoma or foreign bodies[37].

Light-activated therapies

Light-activated therapeutic applications harness the versatility of light in manipulating photoactive molecules, proteins and cells. Phototherapies, which require only an appropriately selected light source, are commonplace in the clinic and are first-line treatments for some conditions. For instance, since the 1960s, blue-light phototherapy has been used to treat severe hyperbilirubinemia in millions of infants[38]. More broadly, the use of exogenous photosensitizers offers capabilities beyond intrinsic light-induced signalling, such as oxidative killing of unwanted cells in photodynamic therapy (PDT). Today, PDT is an established modality used in oncology, dermatology, ophthalmology, dentistry, cosmetics and other fields. The combined global markets for drugs and devices used in phototherapy and PDT were estimated to be US$630 million in 2014 (Fig. 2b).

Ultraviolet light (100–400 nm). Exposure to the Sun's UV radiation, consisting of 95% UVA (320–400 nm) and 5% UVB (290–320 nm), is a major environmental risk factor for skin cancer, which afflicts more than 2 million people worldwide every year. UVB radiation can directly damage DNA, and thus is particularly carcinogenic. UVA can also cause cancer via the generation of DNA-damaging free radicals. Despite the harmful effects, UV-light exposure may have potential beneficial effects through the modulation of immune responses[39]. Indeed, UVB radiation can activate innate immune responses via release of antimicrobial peptides and vitamin D production[40,41], which may play a role in Finsen's phototherapy for lupus vulgaris. UVB light also suppresses the adaptive immune system by activation

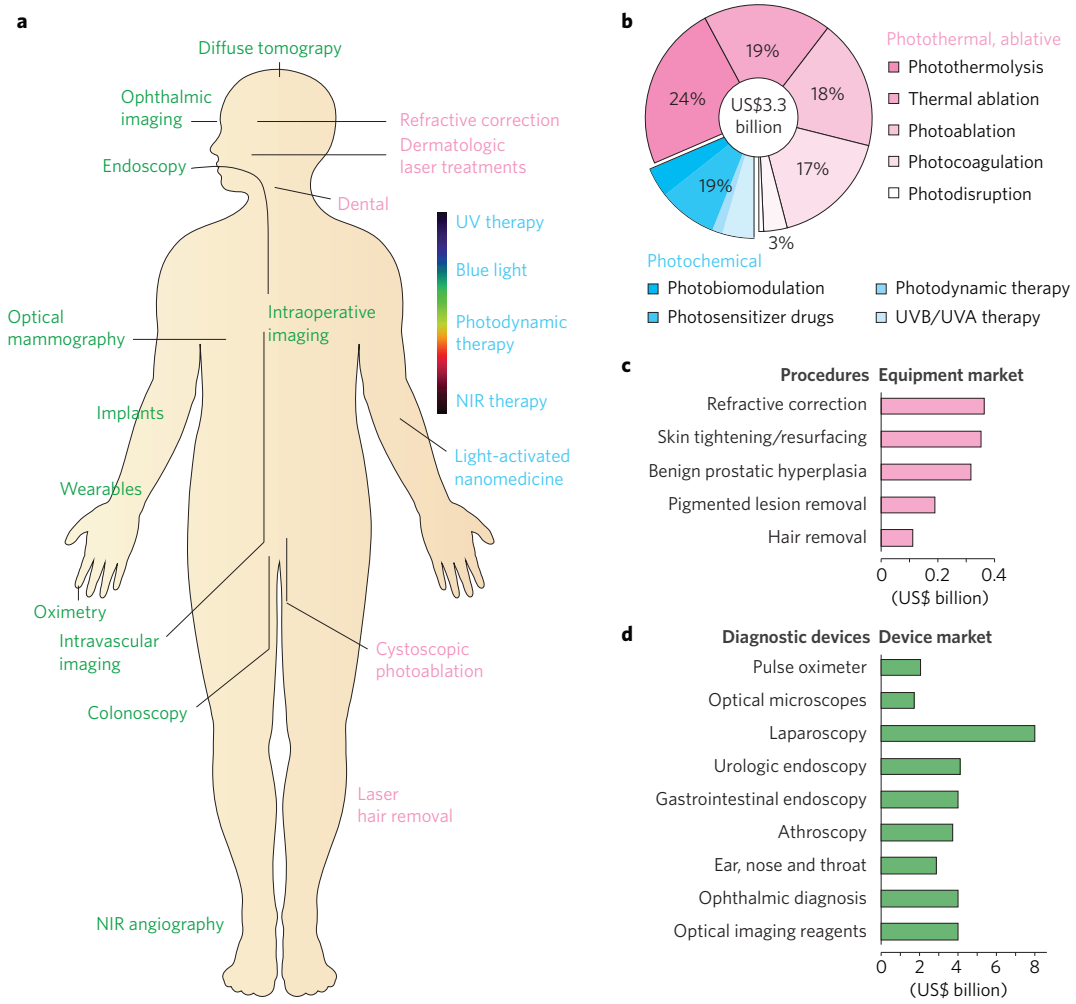

Figure 2 | Medical application areas of light. a, Representative applications of light in the human body for diagnosis and imaging (green), surgery (pink) and therapy (blue). **b**, Global market in 2014 for medical lasers by therapeutic application. **c**, Equipment spending in 2013 for leading laser-treatment procedures. **d**, Global market in 2013–2014 for several major diagnostic devices. Data from BCC Research reports HLC093C, HLC072C and HLC172A (with permission of BCC Research).

of regulatory T cells, B cells and mast cells[42]. UVA light can also be immunosuppressive through the upregulation of the alternative complement pathway[43]. These mechanistic findings have suggested a physiological role for low, non-carcinogenic doses of UV light: induction of innate immunity to protect against microbial attacks, and suppression of adaptive immunity to inhibit autoimmune or allergic responses. The latter mechanism forms the basis of UV phototherapy, which is used to treat a wide range of dermatoses in the clinic[44].

Narrow-band UVB therapy. For over 90 years, UVB radiation has been used to treat psoriasis[44,45] — a chronic, immune-mediated inflammatory skin disorder affecting tens of millions of people worldwide. It is also used to treat vitiligo, atopic dermatitis and other inflammatory dermatoses. With emission at 311 ± 2 nm, narrow-band UVB is preferable to standard broadband UVB (290–320 nm) because of improved efficacy and the reduced risk of erythema (superficial reddening of the skin).

Psoralen and UVA therapy (PUVA). This is another frequent treatment for psoriasis and vitiligo. It requires oral or topical administration of psoralen, exposure to UVA light, and is commonly used to treat patients for whom narrow-band UVB is unsuccessful[46]. The therapy also works through immunosuppressive and antiproliferative effects.

Other effects. Several epidemiology studies have noted that increased sun exposure is associated with decreased risk of multiple sclerosis[47]. A study in mice substantiated these findings, showing that UVB radiation suppresses the progression of experimental autoimmune encephalomyelitis[48]. Another mouse study suggested that UVB radiation may suppress the development of obesity and metabolic syndrome independent of vitamin D supplementation[49].

Visible light (400–700 nm). *Phototherapy for neonatal jaundice.* Jaundiced infants are commonly treated with phototherapy at 460–490 nm, preventing serious sequelae of hyperbilirubinemia, such as permanent neurological damage[38] (Fig. 3e). Blue light isomerizes bilirubin to facilitate its excretion. In the United States, 0.5–4% of term and late-preterm infants receive phototherapy before discharge from the nursery. In low-resource settings, filtered sunlight using canopies is a promising and affordable option for treating neonatal jaundice[50].

Bright light therapy for mood disorders. Seasonal affective disorder is a common form of depression that coincides with shorter days during the winter months and has a prevalence of 0.4–9.9% in the Northern Hemisphere[51]. This disorder and other conditions involving irregular light exposure, such as jet lag, have been linked to mood and cognitive alterations either by modulation of sleep and circadian rhythms, or by

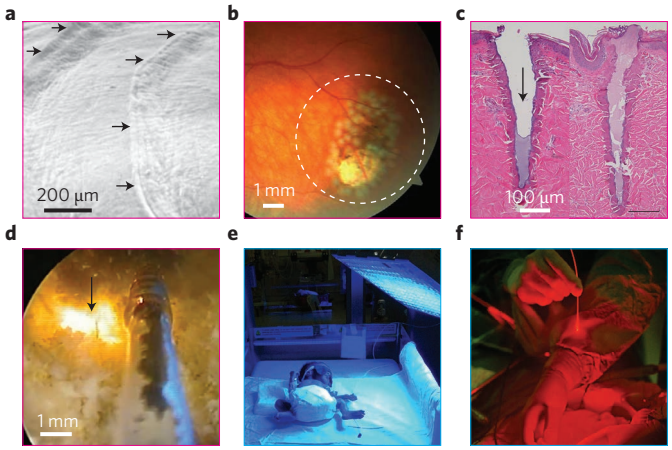

Figure 3 | Surgical and therapeutic applications of light. a, Photoablation. The scanning electron micrograph shows stepwise ablated patterns (arrows) in an experimental cornea by excimer laser irradiation[4]. **b**, Photocoagulation. Laser-induced damage spots around a retinal tear region[7] (dashed circle). **c**, Photothermal ablation. Histology of porcine skin tissues harvested 0 min (left) and 60 min (right) after fractional, pulsed CO_2 laser exposure *in vivo*[16]. The arrow indicates the laser channel, which is filled with a fibrin plug within minutes. **d**, Photothermal ablation (vaporization). A fibre-optic catheter delivers high-power continuous-wave laser light (arrow) to remove excess prostate tissue in a patient with benign prostate hyperplasia (www.youtube.com/watch?v=jAbSwtSN9xE). **e**, Blue-light therapy for the treatment of neonatal jaundice. **f**, Photodynamic therapy. Close-up image of a surgeon's hands in an operating room. Figure reproduced with permission from: **a**, ref. [4], Elsevier; **b**, ref. [7], Digital Journal of Ophthalmology; **c**, ref. [16], Wiley; **d**, Creative Commons licence CC BY 3.0; **e**, Vtbijoy, Creative Commons licence CC BY-SA 3.0; **f**, John Crawford, National Cancer Institute.

direct activation of neural pathways[52]. These mechanisms are mediated by intrinsically photosensitive retinal ganglion cells that express the photopigment melanopsin. Bright-light therapy has proven to be as effective as most antidepressant drugs for treating seasonal affective disorder[53]. In fact, activation of the ganglion cells by bright blue light (480 nm) conveys signals to the brain that suppress melatonin secretion and reset circadian rhythms[54]. Bright-light therapy has also shown promise for the treatment of non-seasonal major depressive disorder[55], but the mechanism of action is still unclear.

Antimicrobial treatment. Antibiotic resistance increasingly threatens the ability to effectively treat bacterial infections. Blue light at 405–470 nm has been effective in treating a broad range of bacterial infections, including *Propionibacterium acnes*-associated acne vulgaris and *Helicobacter pylori* gastritis in humans, as well as wound infections with methicillin-resistant *Staphylococcus aureus* (MRSA) and *Pseudomonas aeruginosa* in mouse models[56,57]. The antimicrobial effect of blue light is thought to arise from the excitation of endogenous porphyrins within the bacterial cells. Before it is accepted for mainstream clinical practice, however, the possible development of microbial resistance to phototherapy needs to be evaluated.

Other effects. Insufficient outdoor exposure to sunlight has been implicated with the growing prevalence of myopia[58] (an estimated 2.5 billion people worldwide will be affected by the condition by 2020). Supporting this observation, high ambient lighting was found to prevent the development of myopia in macaque models[59]. Another potential application is the use of non-ablative lasers to adjuvant vaccines. Pre-treatment of the site of vaccine administration with visible or NIR light significantly enhanced vaccine efficiency and augmented immune responses in mouse models[60].

Near-infrared light (700–1,800 nm). *Photobiomodulation.* Also known as low-level laser-light therapy (LLLT), photobiomodulation uses red and NIR light at 600–1,000 nm, at fluences of 1–10 J cm^{-2} with intensity of 3–90 mW cm^{-2}. Clinical studies have suggested that light can stimulate epidermal stem cells in the hair follicle bulge to promote hair growth[61]. Photobiomodulation for wound healing, tissue repair and anti-inflammatory therapy[62] has been shown to be efficacious in animal models. Results from clinical trials have been mixed, yet have shown therapeutic potential for neck pain[63] and chronic traumatic brain injury[64]. Because its underlying mechanisms are not well understood, adoption of photobiomodulation has been controversial, and its use largely empirical. The mechanisms are largely attributed to the absorption of NIR light by cytochrome C oxidase in mitochondria. This triggers the dissociation of inhibitory nitric oxide from the protein complex, thus increasing adenosine triphosphate synthesis, which can have direct beneficial effects on compromised and hypoxic cells. Therapeutic effects of photobiomodulation may also be mediated by the generation of reactive oxygen species (ROS) and the induction of gene transcription. In fact, photobiomodulation on tooth pulps in rats with 810 nm continuous-wave light at a total dose of 3 J cm^{-2} was shown to form tertiary dentin via direct dental stem cell differentiation through light-induced generation of ROS[65].

Thermal neuromodulation. Optical modulation of neural or muscle activity is increasingly explored as a therapeutic option for neurological and cardiovascular diseases. Thermal neuromodulation by infrared light does not require any exogenous agents or genetic interventions[66]. The mechanism involves absorption of infrared light (1.8–2.2 µm) by water, producing a transient increase in temperature that alters the membrane capacitance and depolarizes the target cell. Pulsed laser light (for example, 0.25 ms and 1–2 J cm^{-2}) has been used to stimulate and control heart beating in intact quail embryos[67] and cranial nerves for nerve monitoring during surgery in gerbil models[68], without causing apparent thermal damage. Although thermal neuromodulation lacks the precision and selectivity afforded by optogenetics, its non-invasive nature could make it more amenable to clinical translation.

Photochemical crosslinking. Photoinduced crosslinking has a variety of applications in biomaterials engineering, biochip fabrication, drug synthesis and dental-composite curing. *In situ* polymerization of UV-epoxy is a common technique in the dental clinic. Corneal collagen crosslinking with riboflavin and UVA light (365 nm; 5 J cm^{-2}) is a treatment for corneal ectasia, such as keratoconus[69] (crosslinking increases the stiffness of corneal stroma by 50–100%). Its application may expand to strengthening a corneal flap, or to refractive error correction by patterned light delivery or multiphoton absorption. Photochemical crosslinking could also be used to bond native collagen fibres to aid wound closure, and to enable the use of photopolymerizable biomaterials as surgical glue[70,71]. In tissue engineering, photopolymerization can be used to fabricate 3D tissue constructs[72], or employed *in situ* to enable restoration of soft tissues[73].

Photodynamic therapy. Three components are required for PDT: a photosensitizer, light energy and oxygen. Following absorption of light by an exogenously delivered photosensitizer, energy is transferred from it to molecular oxygen, generating highly cytotoxic singlet oxygen and ROS. The efficacy of PDT is dependent on its ability to target diseased cells while sparing healthy cells, which requires selective accumulation of the photosensitizer and sufficient delivery of light energy to the target tissue. The antitumour effects of PDT result from the direct killing of tumour cells, the damage to tumour vasculature restricting oxygen and nutrient supply, and the induction of inflammatory responses that can result in

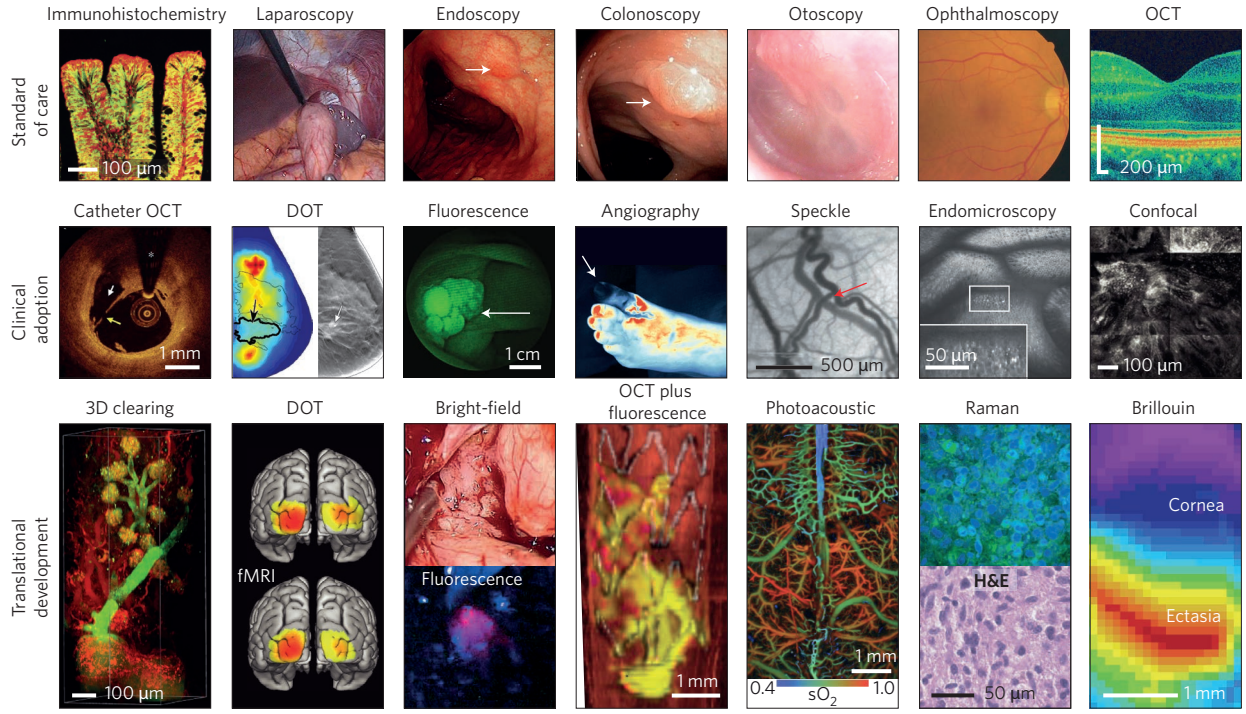

Figure 4 | Current and emerging optical imaging. Top row: established microscopy and endoscopy in routine clinical use. Immunohistochemistry shows c-Met expression in an adenomatous polyp[132]. Laparoscopy visualizes the peritoneal cavity for minimally invasive surgery[148]. Endoscopy reveals a mucosal lesion (arrow) in gastric body[106]. Colonoscopy shows a large, 3-cm sigmoid polyp[107] (arrow). Otoscopy visualizes the eardrum and middle ear[87]. Ophthalmoscopy fundus camera image of the human retina[110]. Optical coherence tomography (OCT) allows microscopic cross-sectional imaging of the retina[110]. Middle row: imaging technologies currently in clinical adoption phases. Catheter OCT shows plaque rupture in a human coronary artery, identified by a broken fibrous cap[113] (arrows). Diffuse optical tomography (DOT; left) combined with X-ray tomosynthesis (right, greyscale) shows oxygen saturation map for a breast with a 2.5-cm malignant tumour[121] (arrows). Fluorescence image shows colorectal polyps labelled with fluorescent peptides[132]. Fluorescence angiography shows loss of blood perfusion (arrow) in the foot[133]. Speckle contrast image reveals meningeal artery (arrow) in the cortex and dura[92]. Confocal laser endomicroscopy shows intramucosal bacteria (bright spots, inset) in the small intestine of a patient with ulcerative colitis[126]. Reflectance confocal microscopy shows an aggregate of neoplastic cells appearing as a focus of bright nuclei in the dermal–epidermal junction[144]. Bottom row: technologies under development or in clinical testing. Microscopy of optically cleared thick-tissue blocks holds promise for the high-content mapping and phenotyping of normal and pathological tissue samples[175]. Functional connectivity maps of three sensory-motor networks generated with high-density DOT and fMRI[122]. Intraoperative imaging of gliomas under white-light and fluorescence imaging with 5-aminolevulinic acid[152]. Multimodal (OCT plus fluorescence) image shows a 3D rendering of the stented right iliac artery of a living rabbit[117]. Red, artery wall; white, stent; purple, thrombus; yellow, NIR fluorescent fibrin. Photoacoustic image of oxygen saturation of haemoglobin (sO_2) in the murine brain vasculature[139]. Clinically viable stimulated Raman microscopy shows hypercellularity and nuclear atypia of tumour, in correspondence with conventional haematoxylin and eosin (H&E) microscopy[138]. Brillouin microscopy shows a longitudinal modulus map of the cornea in a keratoconus patient[146]. Figure adapted with permission from: (top), Immunohistochemistry, ref. [132], Endoscopy, ref. [106], (middle), Fluorescence, ref. [132], Speckle, ref. [92], (bottom), DOT, ref. [122], OCT plus fluorescence, ref. [117], Photoacoustic, ref. [139], Nature Publishing Group; (top), Laparoscopy, ref. [148], Creative Commons licence CC BY 4.0; (bottom), Bright field, ref. [152], Creative Commons licence CC BY 4.0; (top), Colonoscopy, ref. [107], Ophthalmoscopy and OCT, ref. [110], (middle), Catheter OCT, ref. [113], (bottom), 3D clearing, ref. [175], Elsevier; (top) Otoscopy, ref. [87], Massachusetts Medical Society; (middle) Angiography, ref. [133], HMP Communications, LLC; Endomicroscopy, ref. [126], BMJ Publishing Group; Confocal, ref. [144], Wiley; (middle) DOT, ref. [121], Radiological Society of North America; (bottom) Raman, ref. [138], AAAS; Brillouin, ref. [146], American Medical Association.

systemic antitumour immunity[74,75]. Importantly, the mechanisms of cytotoxicity by PDT are fundamentally distinct from those of conventional chemotherapeutics; this may be leveraged in combinatorial therapies of PDT and chemotherapy in order to overcome resistance to cancer drugs[76].

PDT is now clinically approved to treat a number of cancers, including bladder, lung, skin, esophageal, brain, ovarian and bile duct[75] (Fig. 3f). In dermatology, PDT is commonly used for actinic keratosis and acne vulgaris, in addition to superficial non-melanoma skin cancers[77]. PDT is also approved to treat neovascular age-related macular degeneration, but its use has declined since the availability of anti-vascular-endothelial-growth-factor (anti-VEGF) therapy. Outside the clinic, PDT is used to eradicate viruses and other pathogens in blood products. For example, PDT with methylene blue is effective for inactivating viruses, including hepatitis C, HIV-1 and West Nile, and since 1991 it has been used to treat over 4.4 million units of fresh frozen plasma in Europe[78].

The poor penetration depth of visible light required for photosensitizer activation has limited clinical indications of PDT, which is currently only used for the treatment of superficial lesions, or of lesions accessible during surgery or through endoscopy. To extend the therapeutic depth, photosensitizers that can be activated with NIR light are under development[75,79]. Upconversion nanoparticles that convert incident NIR light to visible light for indirect activation of conjugated photosensitizers have shown promise for treating deep-seated and solid tumours in animal models[80]. Another strategy is to deliver bioluminescent molecules directly to target tissues that are inaccessible by external illumination. For example, bioluminescent nanoparticles can activate photosensitizers via resonant energy transfer to treat lymph node metastases in mice[81].

Photothermal therapy. Since the early 1990s, hyperthermic therapy using externally applied radiofrequency, microwave or ultrasound to heat tumours has been used as an adjunct to chemotherapy and radiotherapy to enhance treatment response[82]. In more recent years, the use of thermal agents such as magnetic nanoparticles to selectively localize heat to target tumour cells has shown considerable potential (photothermal therapy can be effective for treating hypoxic tumours, as it does not require oxygen[83]). Strongly absorbing nanoparticles, such as gold nanocages, can induce hyperthermia or thermal ablation. Among NIR-absorbing noble metal nanoparticles utilizing surface plasmon resonances[84], only gold nanoshells have been tested in patients (in ongoing clinical trials for lung and head-and-neck tumours). In fact, the clinical translation of these biodegradable inorganic nanoparticles has been slowed by concerns over their biocompatibility, clearance and long-term toxicity. This has spurred the development of biodegradable organic photothermal agents[85], such as porphysome nanoparticles[86].

Optical diagnostics and imaging

Optical technologies are used along the entire spectrum of diagnostic medicine, from point-of-care and laboratory testing, to screening and diagnostic imaging, to treatment monitoring, to intraoperative imaging. Optical imaging enables real-time visualization of tissues and cells at high spatial resolutions with instrumentation that is relatively inexpensive and portable, especially compared with MRI and CT. A variety of macroscopic and microscopic imaging technologies have been adopted in clinical practice as standard of care, are currently in clinical adoption phases, or are under development for clinical translation (Fig. 4). In the operating room, surgical techniques that rely on optical guidance, such as laparoscopic surgery, have reduced the risk of haemorrhage and shortened patient recovery time. Intraoperative optical imaging provides tissue contrast beyond what can be perceived by the human eye, resulting in improved surgical outcomes. In this section, we discuss optical technologies that have enhanced the physician's ability to screen for, diagnose and monitor disease, with a focus on applications that have addressed previously unmet clinical needs.

Point-of-care testing. Optical technologies are an integral part of patient care, from routine physical examinations to bedside diagnostic testing. Relatively simple instruments such as the otoscope[87] and the ophthalmoscope enhance visual inspection of tissues. Probing light absorption and scattering by tissue constituents enables measurement of important diagnostic indicators, including haemodynamics and the presence of specific biomarkers. The most prominent example is the pulse oximeter, which relies on absorption differences between oxygenated and deoxygenated haemoglobin to estimate the patient's arterial oxygen saturation. Beyond its universal use in emergency medicine, pulse oximetry has also become an effective screening tool for congenital heart defects in newborns[88]. NIR spectroscopy, also relying on haemoglobin absorption, is an emerging tool for non-invasive monitoring of brain function[89]. Spectroscopic techniques sensitive to changes in cellular chromophore concentrations are also being developed for cancer screening, such as for the diagnosis of oral cancer[90]. Dynamic light scattering techniques are increasingly adopted in the clinic for rapid, real-time assessment of microvascular function[91], such as for burn wounds or atherosclerosis. Two techniques relying on NIR laser light scattered by moving red blood cells are laser Doppler imaging, which detects frequency-shifted light, and laser speckle contrast imaging[92], which measures motion-induced intensity fluctuations.

Extensive efforts have been made in the development of optical technologies for point-of-care testing in resource-limited settings[93]. Lens-free computational imaging has eliminated the need for costly optical components, enabling the development of low-cost, portable, on-chip diagnostic platforms[94]. Ubiquitous optical devices such as smartphone cameras may be modified to add diagnostic functionalities such as calorimetric detection[95], multiplexed detection[96], video microscopy[97] and high-resolution spectroscopy[98]. With the continued development of optical technologies, such as fibre optics, optoelectronics and optical microelectromechanical systems, various optical-imaging platforms may be miniaturized for widespread use in point-of-care settings[99].

Molecular diagnostics. Optical techniques have been a mainstay of pathology analysis in the laboratory for over a century. For example, light microscopy is routinely used to analyse peripheral blood smears for haematologic disorders. Flow cytometry, typically through fluorescence-activated cell sorting (FACS), is commonly used for molecular phenotyping of haematologic malignancies and immune disorders, as well as for purifying cellular subpopulations for cell-based therapies. The enzyme-linked immunosorbent assay (ELISA), in which a colour change indicates the binding of specific proteins, is the gold standard for detection of serum antibodies and various biomarkers of disease. To improve sensitivity of protein detection, a number of optical approaches have been proposed, including surface plasmon resonance[100], surface-enhanced Raman scattering[101] and resonant optical cavity sensing[102,103]. Recent innovations in genetic sequencing have ushered in a new era of precision medicine, in which treatment regimens are tailored to patient genotypes. Optical probes are integral tools in genetic analyses, including fluorescence *in situ* hybridization, DNA microarrays and high-throughput sequencing. Future diagnostic tools are likely to combine both optical imaging and sequencing capabilities to fully capture the genetic and phenotypic complexity needed to treat heterogeneous diseases such as cancer[104,105].

Diagnostic imaging. Owing to its non-invasiveness, high-resolution and rich contrast mechanisms, optical imaging is an established and rapidly growing modality for screening and diagnosis. In what follows, we briefly discuss the most clinically relevant optical-imaging methods.

Endoscopy. The standard white-light endoscope is one of the most basic yet essential optical instruments used by physicians to examine the inner organs of patients, such as the gastrointestinal and respiratory tracts[106]. Improvements in optical technologies have greatly enhanced the capabilities of endoscopic imaging, which has coincided with the rapid growth of the endoscopy equipment market (Fig. 2d), projected to reach US$38 billion by 2018. Chromoendoscopy uses dyes or stains to aid tissue characterization such as to identify dysplatic mucosa[107]. Narrow-band imaging, which does not require dyes, relies on the light-penetration difference between blue and green light (typically, 415 and 540 nm) to enhance the visibility of superficial and deeper blood vessels.

Capsule endoscopy. Over the past decade, wireless video capsule endoscopy has become an increasingly popular non-invasive tool for the diagnosis of small bowel disorders[108]. Approved capsule endoscopes consist of a camera sensor, a light-emitting-diode light source, a battery and a wireless radiofrequency transmitter. The capsule is swallowed with water, and excreted with bowel movements. Capsule endoscopes are often the treatment of choice for obscure gastrointestinal bleeding in adults, as they enable the examination of the entire length of the small bowel[109]. They are used increasingly for the assessment of Crohn's disease and for the detection of small bowel tumours.

Ophthalmic imaging. A variety of optical instruments are routinely employed to examine a patient's vision. For example, the slit lamp is used to visualize the anterior and posterior segments of the eye. Rotating the slit illumination in conjunction with a Scheimpflug camera allows for the measurement of corneal topography and of

intraocular pressure by analysing corneal deformation in response to an applied air puff. Other commonly used instruments include wavefront sensors, confocal ophthalmoscopes and fundus cameras. Optical coherence tomography (OCT) is used to obtain high-resolution images of corneal and retina morphology. OCT is the standard of care for diagnosis of pathologies such as glaucoma and age-related macular degeneration[110]. OCT imaging of retinal anatomy is also being explored as a marker for neurological disorders, including multiple sclerosis and Alzheimer's disease.

Optical coherence tomography. OCT is an established modality for high-resolution, label-free, non-invasive imaging[111]. The global market for OCT equipment is growing, and is expected to reach US$1.4 billion by 2019. OCT provides cross-sectional images of tissue microstructure by measuring the echo time delay and intensity of backscattered light at different depths (up to 2–3 mm) at a resolution of 3–15 μm, typically using a broadband light source (800–900 nm) or a wavelength-swept laser (1,200–1,400 nm)[112]. Beyond ophthalmic applications, OCT is clinically approved for catheter-based intracoronary imaging[113], and has been used for the monitoring of outcomes of intracoronary stenting, for assessing coronary plaques in the management of patients with acute coronary syndrome, and for the accurate quantification of fibrous cap thickness as a marker of plaque vulnerability[114]. Another target for OCT is endoscopic imaging of the upper gastrointestinal tract[115]. Technical innovations that may improve the diagnostic capabilities of OCT include cellular resolution[116], high frame rates, birefringence measurement and multimodality[117].

Diffuse optical tomography. Diffuse optical tomography (DOT) is a label-free method that uses NIR light to probe the concentration of haemoglobins, water and lipids in tissues by spectroscopic analysis of optical absorption by these molecules. It has been successful in monitoring the response to neoadjuvant chemotherapy in breast cancer patients[118,119]. Non-responders and responders could be differentiated as early as the first day after chemotherapy, which would allow non-responders to change treatment strategies early, thus avoiding unnecessary toxicities from additional chemotherapy. The chromophore signatures obtained by DOT can also be used to predict the response to neoadjuvant chemotherapy in breast cancer patients prior to treatment[120]. DOT combined with X-ray mammography has shown potential in reducing the false-positive rate of conventional mammography[121]. Recent DOT technology has also enabled functional neuroimaging of the superficial cortex, with images that are of similar quality to those from functional MRI (fMRI)[122]. DOT could thus be advantageous for patients with MRI-incompatible implants or for neonates in intensive care[123].

Fluorescence imaging. Confocal laser endomicroscopy (CLE)[124] uses fluorescence contrast and fibre-bundle probes to generate high-magnification images of the gastrointestinal mucosa. Confocal detection, or collection of fluorescence light only from the illuminated focal plane, enhances spatial resolution compared with conventional endoscopy, enabling assessment of mucosal histology. CLE has shown promise in the detection of neoplasia in patients with Barrett's oesophagus, as well as improved sensitivity over chromoendoscopy in the classification of colorectal polyps[125], in the assessment of inflammatory bowel disease[126] and in the diagnosis of bladder cancer[127]. For molecular imaging, fluorescently labelled peptides that specifically bind to dysplastic tissue have been used to detect colonic dysplasia[128] and esophageal neoplasia[129]. Fluorescent lectins that bind to normal tissue can also be used as negative contrast agents[130]. Although the high resolution of CLE enables accurate image quantification, it is limited by the small field of view, which precludes efficient examination of large areas to detect lesions. This has driven the development of molecular imaging with wide-field fluorescence endoscopy. For example, blue-light cystoscopy with fluorescently labelled CD47 antibodies enabled the detection of bladder cancer in *ex vivo* specimens[131], and neoplastic colorectal polyps in humans were detected through fluorescent peptides targeting c-Met[132]. Recently, fluorescence angiography has been used to visualize tissue perfusion in extremity wounds, such as diabetic foot ulcers[133]. Continued development of molecular imaging agents and optical technologies is likely to fulfil the goal of characterizing lesions *in vivo*, improving diagnostic accuracy and reducing pathology costs.

Nonlinear microscopies. Two-photon microscopy offers the benefit of deeply penetrating NIR light as well as light absorption confined to the focal plane, improving optical sectioning in tissue. However, its use has generally been limited to tissue specimens and small-animal imaging[134] due to the requirement of a femtosecond laser with high peak power. Nonetheless, two-photon microscopy has been used for the diagnosis of malignant melanoma in humans through the imaging of endogenous chromophores[135]. Another target is the non-invasive imaging of retinal pigment epithelium, in particular retinosomes containing fluorescent metabolic products associated with age-related macular degeneration[136]. Nonlinear Raman scattering techniques enable label-free imaging of intrinsic molecular vibrations, generating optical contrast between lipids and proteins[137]. Stimulated Raman scattering microscopy has been used to detect brain-tumour infiltration in fresh specimens from neurosurgical patients, demonstrating near-perfect agreement with standard haematoxylin and eosin light microscopy[138].

Photoacoustic imaging. Photoacoustic or optoacoustic imaging relies on the photoacoustic effect, in which absorption of a periodic train of nanosecond laser pulses induces cyclic, localized heating and cooling, generating pressure waves that can be detected by ultrasound transducers[139]. Its main advantages include enhanced depth penetration compared with optical imaging and multispectral imaging of multiple endogenous or exogenous absorbers. This technique can be readily integrated with commercial ultrasound probes to enhance image contrast through the detection of vasculature or contrast agents[140]. The sensitivity can also be leveraged for the *in vivo* detection of circulating tumour cells in rodent models[141]. In initial patient studies of breast cancer imaging, it has shown promise for the imaging of tumour vasculature and oxygenation with higher spatial resolution than DOT[142,143].

Other techniques. Reflectance confocal microscopy is an accurate non-invasive technique for the diagnosis of basal cell carcinoma[144], and may be able to diagnose melanoma[145]. Brillouin microscopy relies on light scattering from spontaneous acoustic waves in tissue to provide biomechanical information of transparent ocular tissues. It has been used in humans *in vivo* to map stiffness in healthy and keratoconus corneas[146].

Imaging in surgery and therapy. Optical imaging during surgical operation has become increasingly indispensable, guiding the surgeon's eye through narrow endoscopic channels, and providing greater contrast and higher resolution between healthy and diseased tissues than perceived by the naked eye.

Endoscopic imaging. Minimally invasive surgeries, or endoscopic surgeries, have dramatically changed the way operations are performed. In the United States, 96% of cholecystectomies are performed by laparoscopy[147], whereas many other procedures increasingly use minimally invasive techniques[148]. Compared with open procedures, laparoscopic techniques have resulted in superior surgical outcomes due to smaller scars, fewer complications and quicker recovery. Advances in optical devices and technologies have enabled surgeons

to operate effectively without direct visualization of the target tissue. Stereoscopic vision has been employed in precision robotic surgery[149].

Intraoperative imaging. For open-field procedures, surgeons rely on visual inspection and palpation to differentiate between healthy and diseased tissue. However, human vision through white-light reflectance cannot easily discriminate between different tissue types, and is limited by haemoglobin absorption and tissue scattering. For cancer surgeries, the ability to discriminate between malignant and normal tissue is paramount for determining which tissues to resect or preserve. A growing number of clinical trials in recent years have showcased the promise of fluorescence-guided surgery in improving surgical outcomes, decreasing surgical time and lowering overall healthcare costs[150,151].

Fluorescence-guided surgery has been adopted for the resection of high-grade gliomas[152]. Orally administered 5-aminolevulinic acid (ALA) is metabolically activated to form protoporphyrin IX, which accumulates in tumour tissues and exhibits red fluorescence. A phase-III clinical trial showed significantly improved complete resection and higher 6-month progression-free survival when ALA guidance was used instead of white-light illumination[153]. Similarly, ALA has been used to guide tumour resection of bladder cancer, resulting in improved outcomes.

Exogenous NIR fluorescent probes are ideal for intraoperative imaging because of minimal background autofluorescence and enhanced tissue penetration (when compared with visible light). Currently, the only NIR probe approved by the Food and Drug Administration and the European Medicines Agency is indocyanine green (ICG)[151]. Other probes with reduced background[154] and high tissue specificity[155] are under development. The clinical utility of ICG for surgical guidance has been demonstrated for the mapping of sentinel lymph nodes[156] and in the detection of previously undetectable small liver metastases[157].

Molecular imaging. The next frontier for fluorescence-guided surgery involves tumour-targeting, molecular contrast agents. In 2011, the first in-human trial of tumour-specific fluorescence-guided surgery was conducted in patients with ovarian cancer[158]. Using folate–fluorescein isothiocyanate to target folate receptor-α, which is expressed in 90–95% of patients with epithelial ovarian cancer, surgeons were able to identify significantly more tumour deposits than with visual inspection alone. However, folate receptor-α is overexpressed only in certain cancers, which limits the general applicability of folate-conjugated dyes. Another approach currently in development uses activatable probes that become fluorescent when exposed to proteases overexpressed in tumours, thus enabling optical contrast between normal and tumour tissues[159–162]. Labelling peripheral nerves with fluorescent peptides may also prevent accidental transection of nerves during surgery[160].

Table 1 | Emerging medical applications of advanced optical technologies.

Area	Emerging applications
Diagnostic imaging	Non-invasive screening Super-resolution imaging Molecular diagnosis
Health monitoring	Point-of-care testing Implantable devices Mobile health
Surgery	Fluorescence-guided surgery Robotic surgery Intraoperative optical biopsy
Therapy	Targeted therapy Precision medicine Optogenetics

Optical imaging and diagnostic technologies are increasingly less invasive, more accurate, molecular-specific, cost effective and mobile. More surgical procedures will benefit from advanced optical imaging and optimized laser sources. Light-based therapies will integrate nanotechnologies and genetic technologies.

Microscopic and spectroscopic guidance. Although large-field-of-view, fluorescence-based imaging is most suited for surgical guidance in the operating room, optical microscopy techniques with high resolution and reduced field of view have also demonstrated intraoperative utility. OCT has been widely used for ophthalmologic surgeries[163] and in conjunction with angiography for percutaneous coronary intervention[164]. OCT and stimulated Raman scattering microscopy have been used to delineate brain tumours in mice *in vivo*[165,166]. Raman scattering spectroscopy has been used to detect brain cancer cells in humans during brain surgery[167]. Rapid detection of cancer cells by optical methods could therefore become an invaluable tool for surgical decision-making.

Optical imaging in theranostics. Broadly defined, theranostics refers to the combination of therapeutic modalities and diagnostic imaging to adjust treatment protocols to the needs of individual patients. Optical imaging can facilitate the detection of pathologies, the determination of target location and dosimetry, and the monitoring of therapeutic effects *in situ*. Optical imaging is particularly well suited for guiding light-activated therapies, which require light sources. Detection of photosensitizer fluorescence is commonly used for the monitoring and optimization of PDT[168,169]. *In vivo* fluorescence molecular imaging can also be used to predict therapeutic outcomes, as has been shown for cancer[170] and Crohn's disease[171]. And optical Cherenkov emission from radioisotopes could be useful for the dosimetry of X-ray external-beam radiation therapy[172].

Emerging technologies

With the success of medical lasers and optical technologies and the recognition of the needs and opportunities for better healthcare (Table 1), considerable efforts have been made to develop improved or new light-based technologies. Technological innovations continue to push the envelope of optical imaging, including super-resolution imaging beyond the diffraction limit[173] and rapid 3D imaging with light-sheet microscopy[174]. Tissue-clearing techniques that render entire organs optically transparent while preserving tissue microstructure[175] may enhance clinical histological evaluation. Spatial light modulation that counteracts scattering in tissues for improved light penetration and resolution could lead to practical tools for imaging, endoscopy and light-activated therapies[176]. Besides advances in optics and photonics, progress in other fields, such as nanotechnology, bioinspired engineering, genome editing and advanced materials, has opened up opportunities for further innovation in photomedicine. Injectable multifunctional nanoparticles enable light energy to be relayed to specific cells of interest while providing spatiotemporal control of light activation. Genetic integration of fluorescent proteins enables the identification of molecular targets, whereas optogenetics offers precise control of cellular function in the nervous system. These technologies harness the molecular specificity of light–tissue interactions to meet the need for more precise and personalized therapies, such as the targeting of vulnerable cancer cells identified by molecular profiling. At the same time, advances in biomaterials and optoelectronics have led to novel optical devices that can be worn or safely integrated in the human body, allowing continuous health monitoring and providing new opportunities to deliver light to targets previously inaccessible by external illumination.

Light-activated nanomedicine. Nanoparticles based on lipid, polymeric and inorganic materials have advantages over molecular-based

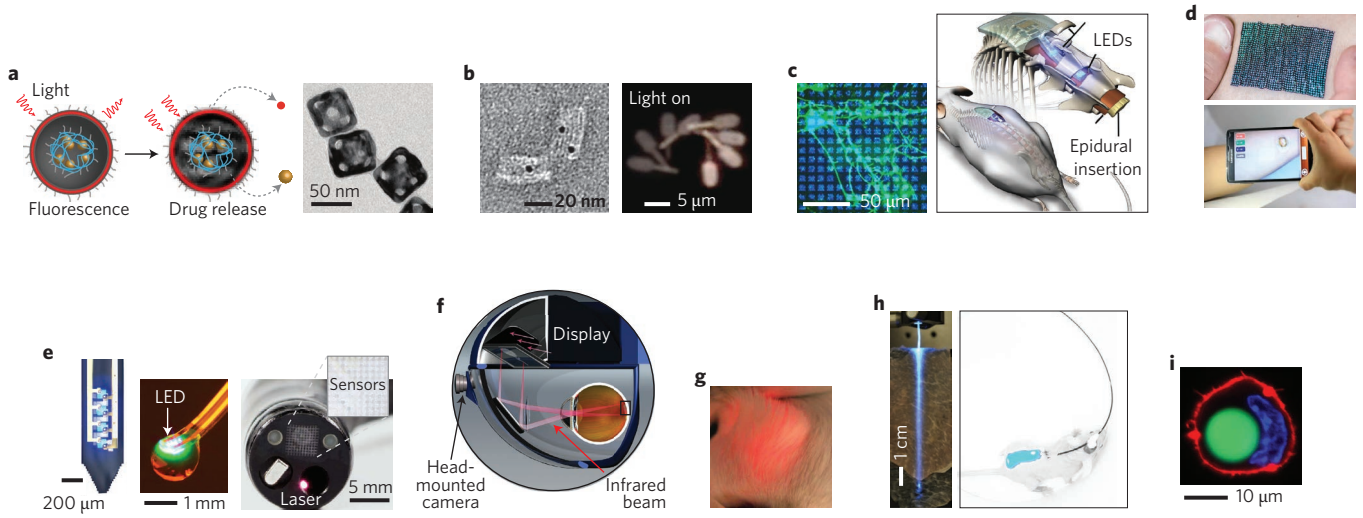

Figure 5 | Various implantable photonic devices at the proof-of-concept stage. a, Nanoparticles for drug delivery and treatment monitoring. Left: light-activated drug release[187]. Right: photothermal-polymer-coated gold nanocages[180]. **b**, Nanorobots. Left: transmission electron microscope image of an aptamer-gated DNA nanorobot capable of transporting 5-nm gold nanoparticles (black dots) to cells[192]. Right: light-controllable microrobot with nanoscale phototactic machinery[194]. **c**, Optogenetic devices. Left: optical pattern illuminated on cultured neuronal cells[204]. Right: miniaturized, wireless, soft optoelectronic systems implanted in the spinal cord for performing optogenetics[223]. **d**, Wearables. Top: thermo-chromic liquid-crystal-based temperature imaging device on the skin[213]. Bottom: epidermal optoelectronic device communicating with a smartphone[217]. **e**, Microprobes. Left: multifunctional, implantable optoelectronic device with LEDs and microelectrodes[221]. Middle: optoelectronic drug-delivery probe[224]. Right: multifunctional endoscope system based on transparent bioelectronic sensors and theranostic nanoparticles[218]. **f**, Vision prosthetics. Retinal prosthetic system using a head-mounted camera and a goggle, which projects NIR (880–915 nm) images to photodiode arrays implanted in the retina[219]. **g**, Wirelessly powered, subcutaneously implanted LED in a mouse[225]. **h**, Biomaterial devices. Left: biodegradable polymer waveguide implanted in tissue for efficient light delivery[229]. Right: fibre-pigtailed hydrogel waveguide implanted in a freely moving mouse for sensing and therapy[212]. **i**, Human cell containing an intracellular fluorescent-bead laser (green)[232]. Figure adapted with permission from: **a** (left), ref. [187], (right), ref. [180], **b** (right), ref. [194], **c** (right), ref. [223], **d** (top), ref. [213], **e** (right), ref. [218], **f**, ref. [219], **g**, ref. [225], **h** (right), ref. [212], **i**, ref. [232], Nature Publishing Group; **b** (left), ref. [192], **e** (left), ref. [221], AAAS; **c** (left), ref. [204], Cambridge Univ. Press; **d** (bottom), ref. [217], AAAS; **e** (middle), ref. [224], Elsevier; **h** (left), ref. [229], Wiley.

therapeutics, such as tunability of size and shape, versatile functionalization capabilities for active targeting and unique optical properties[177]. Light-triggered drug release from nanoparticles enables the on-demand, spatiotemporally controlled delivery of therapeutic agents. This allows dosing regimens to be tailored to patient needs while increasing drug concentration at target tissues and reducing systemic toxicities. For cancer patients, the optimal timing of a chemotherapeutic treatment could enhance antitumour efficacy and reduce metastatic spread[178]. Strategies for nanoparticle-mediated drug delivery include NIR-to-UV light transduction by upconversion nanoparticles[179], NIR-light-induced heating of thermosensitive polymers[180] (Fig. 5a) and permeabilization of drug-containing liposomes[181].

Multifunctional nanoparticles that bear a combination of diagnostic and therapeutic functionalities — theranostic agents — are of particular interest for precision medicine, as they combine both biomarker identification and therapy in a single platform. Theranostic capabilities can span a wide array of modalities, including fluorescence and photoacoustic imaging, PET, MRI, photodynamic and photothermal therapy, and drug delivery[182–186]. The spatiotemporal localization and synchronization of these multimodal therapies can lead to synergistically enhanced therapeutic efficacy. One promising approach is the nanoparticle-mediated combination of PDT and chemotherapy[187,188] (Fig. 5a). Another example takes advantage of clustering of drug-loaded liposomes and antibody-targeted gold nanoparticles inside cancer cells[189]. When exposed to laser light, a plasmonic nanobubble destroys the host cancer cell, ejecting chemotherapeutic drugs and potentiating the effects of X-ray radiation therapy.

A major barrier to systemically administered nanomedicines, particularly for cancer therapy, is the inefficient delivery of nanoparticles to the tumour or target site[190]. Overcoming this barrier will require both improvements in nanoparticle design and better understanding of biological responses to nanoparticle delivery[191]. In future, applications of light-activated nanoparticles are likely to extend beyond imaging and the delivery of direct therapeutic payloads[192]. Indeed, light activation may be useful for modulating biological behaviours at the systems level for therapeutic benefit; for example, NIR-light-induced heating of gold nanorods has been used to cause a clotting cascade in tumours, which then amplified the delivery of chemotherapeutics targeted to a by-product of the coagulation cascade[193]. Another potential avenue is the manipulation of nanorobots to perform complex tasks *in vivo* (such as precise, non-invasive surgeries). Towards this end, a recently developed light-controlled, programmable artificial microswimmer sensed and oriented its migration to the direction of external illumination[194] (Fig. 5b).

Optogenetic therapies. Optogenetics has revolutionized the way light can be used to control cellular activity[195]. In a typical protocol, target cells are rendered photoactive via genetic integration of microbial opsins (light-gated ion channels), thus enabling optical control of electrical activity. Optogenetic techniques have enabled unprecedented insights into disease circuitry, which led to immediate clinical impact. For example, optical dissection of brain circuitry in mouse models revealed mechanisms of deep brain stimulation in the treatment of Parkinson's disease[196], and helped to design new deep-brain-stimulation protocols for treating cocaine addiction[197].

Because of its capabilities for neuromodulation therapy, optogenetics has enticing clinical potential. However, significant barriers to use in the clinic remain, such as the need for genetic transfection and proper illumination[198,199]. Optogenetic therapy for conditions such as depression[200], chronic pain[201] and laryngeal paralysis[202] has been tested in rodent models and may one day be translated

for use in humans. Orphan status was recently granted to a viral-vector-based optogenetic therapy (from RetroSense Therapeutics) for retinitis pigmentosa, and initial clinical trials to evaluate safety are underway. In this case, optogenetic transfection can impart light-sensing ability to relevant cell types (such as ON bipolar cells) located downstream of the damaged photoreceptors[203]. A more recent concept is the coupling of an optogenetic retinal prosthesis with a high-radiance, optical-stimulation display device[204] (Fig. 5c).

A long-term limitation of optogenetic therapies concerns the potential adverse immune responses resulting from the xenotransplantation of microbial proteins into humans. Light-activated control of native ion channels can also be achieved through exogenously delivered caged molecules or photoswitchable compounds[205]. Indeed, photoisomerizable photoswitches have been used to restore visual responses in blind mice[206], and to reversibly control nociception in rats[207]. To enable genetic targeting to specific cells, mammalian ion channels can be engineered to impart light-gated functionality[208], enabling restoration of retinal function in blind mice and dogs[209]. Melanopsin — a mammalian opsin that controls G protein signalling pathways — can also be introduced to render cells photosensitive[210]. These optogenetic tools can create synthetic gene circuits with therapeutic applications. For example, an optogenetic circuit that regulates the expression of glucagon-like peptide-1 was developed for the treatment of type 2 diabetes. When implanted in diabetic mice, the engineered optogenetic cells improved blood-glucose homeostasis on treatment with blue light[211,212]. Therapies involving the implantation of genetically modified cells rather than *in vivo* gene therapy could have an easier path to clinical translation.

Wearable, personal healthcare devices. The skin offers a promising site for measuring physiological information (such as body temperature) for continuous health monitoring[213] (Fig. 5d). The development of low-cost, stretchable and flexible optoelectronics[214,215], such as polymer light-emitting diodes (LEDs), may enable a range of wearable health-monitoring devices in both clinical and at-home settings. Examples include a flexible, all-organic optoelectronic pulse oximeter that has comparable efficiency to commercially available oximeters[216], and a wireless, stretchable optoelectronics device worn on the skin for monitoring blood flow and sweat[217] (Fig. 5d). Future wearable devices could incorporate therapeutic functionalities, such as antibacterial blue-light therapy or low-level light therapy. Flexible optoelectronic devices may also be incorporated into endoscopes for multimodal theranostic functionality[218] (Fig. 5e).

Implantable optoelectronic devices. A significant portion of the more than US$200-billion-per-year global medical device market is for devices that are implanted in the human body. Artificial intraocular lenses make up the largest number of implanted medical devices, accounting for nearly 40% of the market in 2011. Prosthetic retinas promise to restore vision in patients blinded by the degeneration of retinal photoreceptor cells, and their development is being fuelled by advances in optoelectronic technologies (Fig. 5f)[219]. With rapid advances in bio-optic interface technologies and heightened recognition of light versatility in diagnostics and therapies, many new implantable devices based on light-based functionalities are likely to emerge. Novel device concepts and designs include implantable LEDs[220], miniaturized wireless optoelectronic devices for optogenetic applications[221–223] and optofluidic-controlled drug delivery[224] (Fig. 5e). Remotely powered, wireless LED implants offer the potential to enable light-activated therapies in the body. Using radiofrequency[225] or mid-field transmission[226], it is possible to transfer a few milliwatts of electrical power over 10 cm across tissue, sufficient to drive an LED or laser diode for optical sensing and chronic PDT (Fig. 5g). Besides battery or wireless powering, these devices may be self-powered by harnessing kinetic energy from muscular movements[227]. LEDs may also be integrated into existing device platforms, such as gastrointestinal stents[228].

Biomaterial photonic devices. To fully realize the diversity in light–tissue interactions for medical applications, light must be delivered to target tissues with sufficient energy and specificity. Biomaterial waveguides may be used for long-term light delivery[229] and need not be removed if they are made of biodegradable materials, such as silk and poly(L-lactide-co-glycolide)[230] (Fig. 5h). Light-controlled therapy and sensing have been demonstrated by using fibre-optic hydrogel implants with fluorescent reporters and optogenetic cells[212] (Fig. 5h). Multifunctional optical fibres may be implanted for neuromodulation of the nervous system in the body[231]. Cell-based lasers may offer new ways of delivering light by exploiting the intrinsic capabilities of the cells carrying intracellular lasers[232] (Fig. 5i) to target, for example, sites of inflammation, and to permit highly multiplexed imaging based on narrow-band coherent emission[233].

Outlook

Laser surgery and treatments, particularly in dermatology and ophthalmology, are clinically established yet steadily growing areas. Development of new, compact and cost-effective lasers delivering desired output characteristics will expand clinical utilities and enhance treatment outcomes. Phototherapies and photoactivated drug therapies have a long history, yet only a handful of modalities have been adopted as first-line treatments in modern medicine. Nevertheless, recent progress in the understanding of light–tissue interactions, drug delivery and nanotechnologies will accelerate clinical translation. Optical diagnostics and imaging have enjoyed growing clinical adoption in many areas and will find increasing utilities. The wide variety of strategies for enhancing imaging contrast, resolution and molecular specificity make optical imaging a powerful modality, especially in conjunction with conventional radiologic imaging. Given the versatile role of light in nature, the many ways that light-based approaches can sense, monitor and manipulate biological processes is not surprising. In the years to come, increased integration of light-sensitive functionalities in patients through genetic engineering, implantable optoelectronics and intracellular devices such as micro- and nanolasers, will further enrich the role of light in medicine. As noted in 1909 by the radiographer Harvey van Allen[234], "Many other things have been claimed for light treatment, but other methods have proved better in those cases in my hands. We need to look at these things carefully and not be carried away by our enthusiasm." More than a century later, the excitement in photomedicine is still high.

Received 8 May 2016; accepted 10 November 2016;
published 10 January 2017

References

1. Zaret, M. M. *et al.* Ocular lesions produced by an optical maser (laser). *Science* **134,** 1525–1526 (1961).
2. Goldman, L. & Wilson, R. G. Treatment of basal cell epithelioma by laser radiation. *JAMA* **189,** 773–775 (1964).
3. Sakimoto, T., Rosenblatt, M. I. & Azar, D. T. Laser eye surgery for refractive errors. *Lancet* **367,** 1432–1447 (2006).
4. Marshall, J., Trokel, S., Rothery, S. & Krueger, R. Long-term healing of the central cornea after photorefractive keratectomy using an exicmer laser. *Opthalmology* **95,** 1411–1421 (1988).
5. Solomon, K. D. *et al.* LASIK world literature review: quality of life and patient satisfaction. *Ophthalmology* **116,** 691–701 (2009).
6. Palanker, D. V. *et al.* Femtosecond laser-assisted cataract surgery with integrated optical coherence tomography. *Sci. Transl. Med.* **2,** 58ra85 (2010).
7. Karabag, R. Y. Retinal tears and rhegmatogenous retinal detachment after intravitreal injections: its prevalence and case reports. *Digit. J. Ophthalmol.* **21,** 8–10 (2015).

8. Sternberg, P. Subfoveal neovascular lesions in age-related macular degeneration. Guidelines for evaluation and treatment in the macular photocoagulation study. *Arch. Ophthalmol.* **109,** 1242–1257 (1991).
9. Tanzi, E. L., Lupton, J. R. & Alster, T. S. Lasers in dermatology: four decades of progress. *J. Am. Acad. Dermatol.* **49,** 1–34 (2003).
10. Anderson, R. R. & Parrish, J. A. Selective photothermolysis: precise microsurgery by selective absorption of pulsed radiation. *Science* **220,** 524–527 (1983).
11. Anderson, R. R. & Parrish, J. A. Microvasculature can be selectively damaged using dye lasers: a basic theory and experimental evidence in human skin. *Lasers Surg. Med.* **1,** 263–276 (1981).
12. Nelson, J. S. *et al.* Dynamic epidermal cooling during pulsed laser treatment of port-wine stain. A new methodology with preliminary clinical evaluation. *Arch. Dermatol.* **131,** 695–700 (1995).
13. Fitzpatrick, R. E., Goldman, M. P., Satur, N. M. & Tope, W. D. Pulsed carbon dioxide laser resurfacing of photo-aged facial skin. *Arch. Dermatol.* **132,** 395–402 (1996).
14. Manstein, D., Herron, G. S., Sink, R. K., Tanner, H. & Anderson, R. R. Fractional photothermolysis: a new concept for cutaneous remodeling using microscopic patterns of thermal injury. *Lasers Surg. Med.* **34,** 426–438 (2004).
15. Sherling, M. *et al.* Consensus recommendations on the use of an erbium-doped 1,550-nm fractionated laser and its applications in dermatologic laser surgery. *Dermatologic Surg.* **36,** 461–469 (2010).
16. Kositratna, G., Evers, M., Sajjadi, A. & Manstein, D. Rapid fibrin plug formation within cutaneous ablative fractional CO_2 laser lesions. *Lasers Surg. Med.* **48,** 125–132 (2016).
17. Kilmer, S. L. & Anderson, R. R. Clinical use of the Q-switched ruby and the Q-switched Nd:YAG (1064 nm and 532 nm) lasers for treatment of tattoos. *J. Dermatol. Surg. Oncol.* **19,** 330–338 (1993).
18. Brauer, J. A. *et al.* Successful and rapid treatment of blue and green tattoo pigment with a novel picosecond laser. *Arch. Dermatol.* **148,** 820–823 (2012).
19. Grossman, M. C., Dierickx, C., Farinelli, W., Flotte, T. & Anderson, R. R. Damage to hair follicles by normal-mode ruby laser pulses. *J. Am. Acad. Dermatol.* **35,** 889–894 (1996).
20. Metelitsa, A. I. & Green, J. B. Home-use laser and light devices for the skin: an update. *Semin. Cutan. Med. Surg.* **30,** 144–147 (2011).
21. Jackson, S. D. Towards high-power mid-infrared emission from a fibre laser. *Nat. Photon.* **6,** 423–431 (2012).
22. Gilling, P., Cass, C., Cresswell, M. & Fraundorfer, M. Holmium laser resection of the prostate: preliminary results of a new method for the treatment of benign prostatic hyperplasia. *Urology* **47,** 48–51 (1996).
23. Malek, R. S., Kuntzman, R. S. & Barrett, D. M. High-power potassium-titanyl-phosphate (KTP/532) laser vaporization prostatectomy: 24 hours later. *Urology* **51,** 254–256 (1998).
24. Sofer, M. *et al.* Holmium:YAG laser lithotripsy for upper urinary tract calculi in 598 patients. *J. Urol.* **167,** 31–34 (2002).
25. Ell, C., Lux, G., Hochberger, J., Müller, D. & Demling, L. Laser lithotripsy of common bile duct stones. *Gut* **29,** 746–751 (1988).
26. Wazni, O. *et al.* Lead extraction in the contemporary setting: the LExICon study: an observational retrospective study of consecutive laser lead extractions. *J. Am. Coll. Cardiol.* **55,** 579–586 (2010).
27. Wilkoff, B. L. *et al.* Pacemaker lead extraction with the laser sheath: results of the pacing lead extraction with the excimer sheath (PLEXES) trial. *J. Am. Coll. Cardiol.* **33,** 1671–1676 (1999).
28. Grundfest, W. S. *et al.* Laser ablation of human atherosclerotic plaque without adjacent tissue injury. *J. Am. Coll. Cardiol.* **5,** 929–933 (1985).
29. Min, R. J., Khilnani, N. & Zimmet, S. E. Endovenous laser treatment of saphenous vein reflux: long-term results. *J. Vasc. Interv. Radiol.* **14,** 991–996 (2003).
30. Proebstle, T. M., Moehler, T. & Herdemann, S. Reduced recanalization rates of the great saphenous vein after endovenous laser treatment with increased energy dosing: definition of a threshold for the endovenous fluence equivalent. *J. Vasc. Surg.* **44,** 834–839 (2006).
31. Mccoppin, H. H., Hovenic, W. W. & Wheeland, R. G. Laser treatment of superficial leg veins. *Dermatologic Surg.* **37,** 729–741 (2011).
32. Hibst, R. & Keller, U. Experimental studies of the application of the Er:YAG laser on dental hard substances: I. Measurement of the ablation rate. *Lasers Surg. Med.* **9,** 338–344 (1989).
33. Wigdor, H. A. *et al.* Lasers in dentistry. *Lasers Surg. Med.* **16,** 103–133 (1995).
34. Strong, M. S. & Jako, G. J. Laser surgery in the larynx. Early clinical experience with continuous CO_2 laser. *Ann. Otol. Rhinol. Laryngol.* **81,** 792–798 (1972).
35. Amin, Z. *et al.* Hepatic metastases: interstitial laser photocoagulation with real-time US monitoring and dynamic CT evaluation of treatment. *Radiology* **187,** 339–347 (1993).
36. Mellow, M. H. & Pinkas, H. Endoscopic laser therapy for malignancies affecting the esophagus and gastroesophageal junction: analysis of technical and functional efficacy. *Arch. Intern. Med.* **145,** 1443–1446 (1985).
37. Wahidi, M. M., Herth, F. J. F. & Ernst, A. State of the art: interventional pulmonology. *Chest* **131,** 261–274 (2007).
38. Maisels, M. J. & McDonagh, A. F. Phototherapy for neonatal jaundice. *N. Engl. J. Med.* **358,** 920–928 (2008).
39. Schwarz, T. & Beissert, S. Milestones in photoimmunology. *J. Invest. Dermatol.* **133,** E7–E10 (2013).
40. Gläser, R. *et al.* UV-B radiation induces the expression of antimicrobial peptides in human keratinocytes *in vitro* and *in vivo*. *J. Allergy Clin. Immunol.* **123,** 1117–1123 (2009).
41. Liu, P. T. *et al.* Toll-like receptor triggering of a vitamin D-mediated human antimicrobial response. *Science* **311,** 1770–1773 (2006).
42. Kripke, M. L. Antigenicity of murine skin tumors induced by ultraviolet light. *J. Natl Cancer Inst.* **53,** 1333–1336 (1974).
43. Stapelberg, M. P. F., Williams, R. B. H., Byrne, S. N. & Halliday, G. M. The alternative complement pathway seems to be a UVA sensor that leads to systemic immunosuppression. *J. Invest. Dermatol.* **129,** 2694–2701 (2009).
44. Lim, H. W. *et al.* Phototherapy in dermatology: a call for action. *J. Am. Acad. Dermatol.* **72,** 1078–1080 (2015).
45. Johnson-Huang, L. M. *et al.* Effective narrow-band UVB radiation therapy suppresses the IL-23/IL-17 axis in normalized psoriasis plaques. *J. Invest. Dermatol.* **130,** 2654–2663 (2010).
46. Stern, R. S. Psoralen and ultraviolet A light therapy for psoriasis. *N. Engl. J. Med.* **357,** 682–690 (2007).
47. Norval, M. & Halliday, G. M. The consequences of UV-induced immunosuppression for human health. *Photochem. Photobiol.* **87,** 965–977 (2011).
48. Becklund, B. R., Severson, K. S., Vang, S. V & DeLuca, H. F. UV radiation suppresses experimental autoimmune encephalomyelitis independent of vitamin D production. *Proc. Natl Acad. Sci. USA* **107,** 6418–6423 (2010).
49. Geldenhuys, S. *et al.* Ultraviolet radiation suppresses obesity and symptoms of metabolic syndrome independently of vitamin D in mice fed a high-fat diet. *Diabetes* **63,** 3759–3769 (2014).
50. Slusher, T. M. *et al.* A randomized trial of phototherapy with filtered sunlight in African neonates. *N. Engl. J. Med.* **373,** 1115–1124 (2015).
51. Anderson, J. L., Glod, C. A., Dai, J., Cao, Y. & Lockley, S. W. Lux vs. wavelength in light treatment of seasonal affective disorder. *Acta Psychiatr. Scand.* **120,** 203–212 (2009).
52. LeGates, T. A., Fernandez, D. C. & Hattar, S. Light as a central modulator of circadian rhythms, sleep and affect. *Nat. Rev. Neurosci.* **15,** 443–454 (2014).
53. Golden, R. N. *et al.* The efficacy of light therapy in the treatment of mood disorders: a review and meta-analysis of the evidence. *Am. J. Psychiatry* **162,** 656–662 (2005).
54. Lockley, S. W., Brainard, G. C. & Czeisler, C. A. High sensitivity of the human circadian melatonin rhythm to resetting by short wavelength light. *J. Clin. Endocrinol. Metab.* **88,** 4502–4505 (2003).
55. Lam, R. W. *et al.* Efficacy of bright light treatment, fluoxetine, and the combination in patients with nonseasonal major depressive disorder. *JAMA Psychiatry* **73,** 56–63 (2015).
56. Dai, T. *et al.* Blue light rescues mice from potentially fatal *Pseudomonas aeruginosa* burn infection: efficacy, safety, and mechanism of action. *Antimicrob. Agents Chemother.* **57,** 1238–1245 (2013).
57. Dai, T. *et al.* Blue light for infectious diseases: *Propionibacterium acnes*, *Helicobacter pylori*, and beyond? *Drug Resist. Updates* **15,** 233–236 (2012).
58. Wu, P. C., Tsai, C. L., Wu, H. L., Yang, Y. H. & Kuo, H. K. Outdoor activity during class recess reduces myopia onset and progression in school children. *Ophthalmology* **120,** 1080–1085 (2013).
59. Smith, E. L., Hung, L. F. & Huang, J. Protective effects of high ambient lighting on the development of form-deprivation myopia in rhesus monkeys. *Investig. Ophthalmol. Vis. Sci.* **53,** 421–428 (2012).
60. Wang, J., Li, B. & Wu, M. X. Effective and lesion-free cutaneous influenza vaccination. *Proc. Natl Acad. Sci. USA* **112,** 5005–5010 (2015).
61. Avci, P., Gupta, G. K., Clark, J., Wikonkal, N. & Hamblin, M. R. Low-level laser (light) therapy (LLLT) for treatment of hair loss. *Lasers Surg. Med. Surg. Med.* **46,** 144–151 (2014).
62. Chung, H. *et al.* The nuts and bolts of low-level laser (light) therapy. *Ann. Biomed. Eng.* **40,** 516–533 (2012).
63. Chow, R. T., Johnson, M. I., Lopes-Martins, R. A. & Bjordal, J. M. Efficacy of low-level laser therapy in the management of neck pain: a systematic review and meta-analysis of randomised placebo or active-treatment controlled trials. *Lancet* **374,** 1897–1908 (2009).
64. Naeser, M. A. *et al.* Significant improvements in cognitive performance post-transcranial, red/near-infrared light-emitting diode treatments in chronic, mild traumatic brain injury: open-protocol study. *J. Neurotrauma* **31,** 1008–1017 (2014).
65. Arany, P. R. *et al.* Photoactivation of endogenous latent transforming growth factor-β1 directs dental stem cell differentiation for regeneration. *Sci. Transl. Med.* **6,** 238ra69 (2014).

66. Shapiro, M. G., Homma, K., Villarreal, S., Richter, C.-P. & Bezanilla, F. Infrared light excites cells by changing their electrical capacitance. *Nat. Commun.* **3,** 736 (2012).
67. Jenkins, M. W. *et al.* Optical pacing of the embryonic heart. *Nat. Photon.* **4,** 623–626 (2010).
68. Teudt, I. U., Nevel, A. E., Izzo, A. D., Walsh, J. T. & Richter, C.-P. Optical stimulation of the facial nerve: a new monitoring technique? *Laryngoscope* **117,** 1641–1647 (2007).
69. Wollensak, G., Spoerl, E. & Seiler, T. Stress-strain measurements of human and porcine corneas after riboflavin-ultraviolet-A-induced cross-linking. *J. Cataract Refract. Surg.* **29,** 1780–1785 (2003).
70. Lang, N. *et al.* A blood-resistant surgical glue for minimally invasive repair of vessels and heart defects. *Sci. Transl. Med.* **6,** 218ra6 (2014).
71. Roche, E. T. *et al.* A light-reflecting balloon catheter for atraumatic tissue defect repair. *Sci. Transl. Med.* **7,** 306ra149 (2015).
72. Du, Y., Lo, E., Ali, S. & Khademhosseini, A. Directed assembly of cell-laden microgels for fabrication of 3D tissue constructs. *Proc. Natl Acad. Sci. USA* **105,** 9522–9527 (2008).
73. Hillel, A. T. *et al.* Photoactivated composite biomaterial for soft tissue restoration in rodents and in humans. *Sci. Transl. Med.* **3,** 93ra67 (2011).
74. Castano, A. P., Mroz, P. & Hamblin, M. R. Photodynamic therapy and anti-tumour immunity. *Nat. Rev. Cancer* **6,** 535–545 (2006).
75. Agostinis, P. *et al.* Photodynamic therapy of cancer: an update. *CA Cancer J. Clin.* **61,** 250–281 (2011).
76. Spring, B. Q., Rizvi, I., Xu, N. & Hasan, T. The role of photodynamic therapy in overcoming cancer drug resistance. *Photochem. Photobiol. Sci.* **14,** 1476–1491 (2015).
77. Wan, M. T. & Lin, J. Y. Current evidence and applications of photodynamic therapy in dermatology. *Clin. Cosmet. Investig. Dermatol.* **7,** 145–163 (2014).
78. Lozano, M., Cid, J. & Müller, T. H. Plasma treated with methylene blue and light: clinical efficacy and safety profile. *Transfus. Med. Rev.* **27,** 235–240 (2013).
79. Yang, Y. *et al.* Thienopyrrole-expanded BODIPY as a potential NIR photosensitizer for photodynamic therapy. *Chem. Commun.* **49,** 3940–3942 (2013).
80. Idris, N. M. *et al. In vivo* photodynamic therapy using upconversion nanoparticles as remote-controlled nanotransducers. *Nat. Med.* **18,** 1580–1585 (2012).
81. Kim, Y. R. *et al.* Bioluminescence-activated deep-tissue photodynamic therapy of cancer. *Theranostics* **5,** 805–817 (2015).
82. Hildebrandt, B. The cellular and molecular basis of hyperthermia. *Crit. Rev. Oncol. Hematol.* **43,** 33–56 (2002).
83. Jin, C. S., Lovell, J. F., Chen, J. & Zheng, G. Ablation of hypoxic tumors with dose-equivalent photothermal, but not photodynamic, therapy using a nanostructured porphyrin assembly. *ACS Nano* **7,** 2541–2550 (2013).
84. Huang, X., El-Sayed, I. H., Qian, W. & El-Sayed, M. A. Cancer cell imaging and photothermal therapy in the near-infrared region by using gold nanorods. *J. Am. Chem. Soc.* **128,** 2115–2120 (2006).
85. Cheng, L., Yang, K., Chen, Q. & Liu, Z. Organic stealth nanoparticles for highly effective *in vivo* near-infrared photothermal therapy of cancer. *ACS Nano* **6,** 5605–5613 (2012).
86. Lovell, J. F. *et al.* Porphysome nanovesicles generated by porphyrin bilayers for use as multimodal biophotonic contrast agents. *Nat. Mater.* **10,** 324–332 (2011).
87. Shaikh, N., Hoberman, A., Kaleida, P. H., Ploof, D. L. & Paradise, J. L. Diagnosing otitis media — otoscopy and cerumen removal. *N. Engl. J. Med.* **362,** e62 (2010).
88. Thangaratinam, S., Brown, K., Zamora, J., Khan, K. S. & Ewer, A. K. Pulse oximetry screening for critical congenital heart defects in asymptomatic newborn babies: a systematic review and meta-analysis. *Lancet* **379,** 2459–2464 (2012).
89. Boas, D. A., Elwell, C. E., Ferrari, M. & Taga, G. Twenty years of functional near-infrared spectroscopy: introduction for the special issue. *Neuroimage* **85,** 1–5 (2014).
90. Schwarz, R. A. *et al.* Noninvasive evaluation of oral lesions using depth-sensitive optical spectroscopy. *Cancer* **115,** 1669–1679 (2009).
91. Humeau-Heurtier, A., Guerreschi, E., Abraham, P. & Mahé, G. Relevance of laser doppler and laser speckle techniques for assessing vascular function: state of the art and future trends. *IEEE Trans. Biomed. Eng.* **60,** 659–666 (2013).
92. Bolay, H. *et al.* Intrinsic brain activity triggers trigeminal meningeal afferents in a migraine model. *Nat. Med.* **8,** 136–142 (2002).
93. Boppart, S. A. & Richards-Kortum, R. Point-of-care and point-of-procedure optical imaging technologies for primary care and global health. *Sci. Transl. Med.* **6,** 253rv2 (2014).
94. Greenbaum, A. *et al.* Wide-field computational imaging of pathology slides using lens-free on-chip microscopy. *Sci. Transl. Med.* **6,** 267ra175 (2014).
95. Shen, L., Hagen, J. A. & Papautsky, I. Point-of-care colorimetric detection with a smartphone. *Lab Chip* **12,** 4240–4243 (2012).
96. Ming, K. *et al.* Integrated quantum dot barcode smartphone optical device for wireless multiplexed diagnosis of infected patients. *ACS Nano* **9,** 3060–3074 (2015).
97. Ambrosio, M. V. D. *et al.* Point-of-care quantification of blood-borne filarial parasites with a mobile phone microscope. *Sci. Transl. Med.* **7,** 286re4 (2015).
98. Bao, J. & Bawendi, M. G. A colloidal quantum dot spectrometer. *Nature* **523,** 67–70 (2013).
99. Shelton, R. L. *et al.* Optical coherence tomography for advanced screening in the primary care office. *J. Biophotonics* **7,** 525–533 (2014).
100. de la Rica, R. & Stevens, M. M. Plasmonic ELISA for the ultrasensitive detection of disease biomarkers with the naked eye. *Nat. Nanotech.* **8,** 1759–1764 (2012).
101. Chen, Z. *et al.* Protein microarrays with carbon nanotubes as multicolor Raman labels. *Nat. Biotechnol.* **26,** 1285–1292 (2008).
102. Armani, A. M., Kulkarni, R. P., Fraser, S. E., Flagan, R. C. & Vahala, K. J. Detection with optical microcavities. *Science* **317,** 783–787 (2007).
103. Fan, X. & Yun, S.-H. The potential of optofluidic biolasers. *Nat. Methods* **11,** 141–147 (2014).
104. Crosetto, N., Bienko, M. & van Oudenaarden, A. Spatially resolved transcriptomics and beyond. *Nat. Rev. Genet.* **16,** 57–66 (2015).
105. Friedman, A. A., Letai, A., Fisher, D. E. & Flaherty, K. T. Precision medicine for cancer with next-generation functional diagnostics. *Nat. Rev. Cancer* **15,** 747–756 (2015).
106. Veitch, A. M., Uedo, N., Yao, K. & East, J. E. Optimizing early upper gastrointestinal cancer detection at endoscopy. *Nat. Rev. Gastroenterol. Hepatol.* **12,** 660–667 (2015).
107. Deepak, P. *et al.* Incremental diagnostic yield of chromoendoscopy and outcomes in inflammatory bowel disease patients with a history of colorectal dysplasia on white-light endoscopy. *Gastrointest. Endosc.* **83,** 1005–1012 (2016).
108. Iddan, G., Meron, G., Glukhovsky, A. & Swain, P. Wireless capsule endoscopy. *Nature* **405,** 417 (2000).
109. Liao, Z., Gao, R., Xu, C. & Li, Z.-S. Indications and detection, completion, and retention rates of small-bowel capsule endoscopy: a systematic review. *Gastrointest. Endosc.* **71,** 280–286 (2010).
110. Drexler, W. & Fujimoto, J. G. State-of-the-art retinal optical coherence tomography. *Prog. Retin. Eye Res.* **27,** 45–88 (2008).
111. Huang, D. *et al.* Optical coherence tomography. *Science* **254,** 1178–1181 (1991).
112. Yun, S. H. *et al.* Comprehensive volumetric optical microscopy *in vivo*. *Nat. Med.* **12,** 1429–1433 (2006).
113. Tearney, G. J. *et al.* Consensus standards for acquisition, measurement, and reporting of intravascular optical coherence tomography studies: a report from the International Working Group for Intravascular Optical Coherence Tomography Standardization and Validation. *J. Am. Coll. Cardiol.* **59,** 1058–1072 (2012).
114. Prati, F. *et al.* Expert review document part 2: methodology, terminology and clinical applications of optical coherence tomography for the assessment of interventional procedures. *Eur. Heart J.* **33,** 2513–2520 (2012).
115. Bouma, B. E., Tearney, G. J., Compton, C. C. & Nishioka, N. S. High-resolution imaging of the human esophagus and stomach *in vivo* using optical coherence tomography. *Gastrointest. Endosc.* **51,** 467–474 (2000).
116. Liu, L. *et al.* Imaging the subcellular structure of human coronary atherosclerosis using micro-optical coherence tomography. *Nat. Med.* **17,** 1010–1014 (2011).
117. Yoo, H. *et al.* Intra-arterial catheter for simultaneous microstructural and molecular imaging *in vivo*. *Nat. Med.* **17,** 1680–1684 (2011).
118. Roblyer, D. *et al.* Optical imaging of breast cancer oxyhemoglobin flare correlates with neoadjuvant chemotherapy response one day after starting treatment. *Proc. Natl Acad. Sci. USA* **108,** 14626–14631 (2011).
119. Schaafsma, B. E. *et al.* Optical mammography using diffuse optical spectroscopy for monitoring tumor response to neoadjuvant chemotherapy in women with locally advanced breast cancer. *Clin. Cancer Res.* **21,** 577–584 (2015).
120. Jiang, S. *et al.* Predicting breast tumor response to neoadjuvant chemotherapy with diffuse optical spectroscopic tomography prior to treatment. *Clin. Cancer Res.* **20,** 6006–6015 (2014).
121. Fang, Q. *et al.* Combined optical and X-ray tomosynthesis breast imaging. *Radiology* **258,** 89–97 (2011).
122. Eggebrecht, A. T. *et al.* Mapping distributed brain function and networks with diffuse optical tomography. *Nat. Photon.* **8,** 448–454 (2014).
123. White, B. R., Liao, S. M., Ferradal, S. L., Inder, T. E. & Culver, J. P. Bedside optical imaging of occipital resting-state functional connectivity in neonates. *Neuroimage* **59,** 2529–2538 (2012).
124. Kiesslich, R. *et al.* Confocal laser endoscopy for diagnosing intraepithelial neoplasias and colorectal cancer *in vivo*. *Gastroenterology* **127,** 706–713 (2004).
125. Buchner, A. M. *et al.* Comparison of probe-based confocal laser endomicroscopy with virtual chromoendoscopy for classification of colon polyps. *Gastroenterology* **138,** 834–842 (2010).

126. Moussata, D. *et al.* Confocal laser endomicroscopy is a new imaging modality for recognition of intramucosal bacteria in inflammatory bowel disease *in vivo*. *Gut* **60,** 26–33 (2011).
127. Sonn, G. A. *et al.* Optical biopsy of human bladder neoplasia with *in vivo* confocal laser endomicroscopy. *J. Urol.* **182,** 1299–1305 (2009).
128. Hsiung, P.-L. *et al.* Detection of colonic dysplasia *in vivo* using a targeted heptapeptide and confocal microendoscopy. *Nat. Med.* **14,** 454–458 (2008).
129. Sturm, M. B. *et al.* Targeted imaging of esophageal neoplasia with a fluorescently labeled peptide: first-in-human results. *Sci. Transl. Med.* **5,** 184ra61 (2013).
130. Bird-Lieberman, E. L. *et al.* Molecular imaging using fluorescent lectins permits rapid endoscopic identification of dysplasia in Barrett's esophagus. *Nat. Med.* **18,** 315–321 (2012).
131. Pan, Y. *et al.* Endoscopic molecular imaging of human bladder cancer using a CD47 antibody. *Sci. Transl. Med.* **6,** 260ra148 (2014).
132. Burggraaf, J. *et al.* Detection of colorectal polyps in humans using an intravenously administered fluorescent peptide targeted against c-Met. *Nat. Med.* **21,** 955–961 (2015).
133. Fitzgerald, R. Assessing the potential impact of fluorescence angiography in preventing limb loss. *Pod. Today* **29,** http://www.podiatrytoday.com/assessing-potential-impact-fluorescence-angiography-preventing-limb-loss (2016).
134. Choi, M., Kwok, S. J. J. & Yun, S. H. *In vivo* fluorescence microscopy: lessons from observing cell behavior in their native environment. *Physiology* **30,** 40–49 (2015).
135. Dimitrow, E. *et al.* Sensitivity and specificity of multiphoton laser tomography for *in vivo* and *ex vivo* diagnosis of malignant melanoma. *J. Invest. Dermatol.* **129,** 1752–1758 (2009).
136. Palczewska, G. *et al.* Noninvasive two-photon microscopy imaging of mouse retina and retinal pigment epithelium through the pupil of the eye. *Nat. Med.* **20,** 785–789 (2014).
137. Saar, B. G. *et al.* Video-rate molecular imaging *in vivo* with stimulated Raman scattering. *Science* **330,** 1368–1370 (2010).
138. Ji, M. *et al.* Detection of human brain tumor infiltration with quantitative stimulated Raman scattering microscopy. *Sci. Transl. Med.* **7,** 309ra163 (2015).
139. Yao, J. *et al.* High-speed label-free functional photoacoustic microscopy of mouse brain in action. *Nat. Methods* **12,** 407–410 (2015).
140. Yang, J.-M. *et al.* Simultaneous functional photoacoustic and ultrasonic endoscopy of internal organs *in vivo*. *Nat. Med.* **18,** 1297–1302 (2012).
141. Galanzha, E. I. *et al. In vivo* magnetic enrichment and multiplex photoacoustic detection of circulating tumour cells. *Nat. Nanotech.* **4,** 855–860 (2009).
142. Ermilov, S. A. *et al.* Laser optoacoustic imaging system for detection of breast cancer. *J. Biomed. Opt.* **14,** 24007 (2009).
143. Kitai, T. *et al.* Photoacoustic mammography: initial clinical results. *Breast Cancer* **21,** 146–153 (2014).
144. Scope, A. *et al. In vivo* reflectance confocal microscopy of shave biopsy wounds: feasibility of intraoperative mapping of cancer margins. *Br. J. Dermatol.* **163,** 1218–1228 (2010).
145. Guitera, P. *et al. In vivo* confocal microscopy for diagnosis of melanoma and basal cell carcinoma using a two-step method: analysis of 710 consecutive clinically equivocal cases. *J. Invest. Dermatol.* **132,** 2386–2394 (2012).
146. Scarcelli, G., Besner, S., Pineda, R., Kalout, P. & Yun, S. H. *In vivo* biomechanical mapping of normal and keratoconus corneas. *JAMA Ophthalmol.* **133,** 480–482 (2015).
147. Tsui, C., Klein, R. & Garabrant, M. Minimally invasive surgery: national trends in adoption and future directions for hospital strategy. *Surg. Endosc. Other Interv. Tech.* **27,** 2253–2257 (2013).
148. Omata, J. *et al.* Acute gastric volvulus associated with wandering spleen in an adult treated laparoscopically after endoscopic reduction: a case report. *Surg. Case Reports* **2,** 47 (2016).
149. Jourdan, I. C. *et al.* Stereoscopic vision provides a significant advantage for precision robotic laparoscopy. *Br. J. Surg.* **91,** 879–885 (2004).
150. Vahrmeijer, A. L., Hutteman, M., van der Vorst, J. R., van de Velde, C. J. H. & Frangioni, J. V. Image-guided cancer surgery using near-infrared fluorescence. *Nat. Rev. Clin. Oncol.* **10,** 507–518 (2013).
151. Nguyen, Q. T. & Tsien, R. Y. Fluorescence-guided surgery with live molecular navigation—a new cutting edge. *Nat. Rev. Cancer* **13,** 653–662 (2013).
152. Widhalm, G. *et al.* 5-Aminolevulinic acid induced fluorescence is a powerful intraoperative marker for precise histopathological grading of gliomas with non-significant contrast-enhancement. *PLoS ONE* **8,** e76988 (2013).
153. Stummer, W. *et al.* Fluorescence-guided surgery with 5-aminolevulinic acid for resection of malignant glioma: a randomised controlled multicentre phase III trial. *Lancet Oncol.* **7,** 392–401 (2006).
154. Choi, H. S. *et al.* Targeted zwitterionic near-infrared fluorophores for improved optical imaging. *Nat. Biotechnol.* **31,** 148–153 (2013).
155. Hyun, H. *et al.* Structure-inherent targeting of near-infrared fluorophores for parathyroid and thyroid gland imaging. *Nat. Med.* **21,** 192–197 (2015).
156. Verbeek, F. P. R. *et al.* Near-infrared fluorescence sentinel lymph node mapping in breast cancer: a multicenter experience. *Breast Cancer Res. Treat.* **143,** 333–342 (2014).
157. Van Der Vorst, J. R. *et al.* Near-infrared fluorescence-guided resection of colorectal liver metastases. *Cancer* **119,** 3411–3418 (2013).
158. van Dam, G. M. *et al.* Intraoperative tumor-specific fluorescence imaging in ovarian cancer by folate receptor-α targeting: first in-human results. *Nat. Med.* **17,** 1315–1319 (2011).
159. Metildi, C. A. *et al.* Ratiometric activatable cell-penetrating peptides label pancreatic cancer, enabling fluorescence-guided surgery, which reduces metastases and recurrence in orthotopic mouse models. *Ann. Surg. Oncol.* **22,** 2082–2087 (2014).
160. Whitney, M. A. *et al.* Fluorescent peptides highlight peripheral nerves during surgery in mice. *Nat. Biotechnol.* **29,** 352–356 (2011).
161. Weissleder, R., Tung, C. H., Mahmood, U. & Bogdanov, A. *In vivo* imaging of tumors with protease-activated near-infrared fluorescent probes. *Nat. Biotechnol.* **17,** 375–378 (1999).
162. Whitley, M. J. *et al.* A mouse-human phase 1 co-clinical trial of a protease-activated fluorescent probe for imaging cancer. *Sci. Transl. Med.* **8,** 320ra4 (2016).
163. Ehlers, J. P. *et al.* The prospective intraoperative and perioperative ophthalmic imaging with optical coherence tomography (PIONEER) study: 2-year results. *Am. J. Ophthalmol.* **158,** 999–1007 (2014).
164. Prati, F. *et al.* Angiography alone versus angiography plus optical coherence tomography to guide decision-making during percutaneous coronary intervention: the Centro per la Lotta contro l'Infarto-Optimisation of Percutaneous Coronary Intervention (CLI-OPCI) study. *EuroIntervention* **8,** 823–829 (2012).
165. Kut, C. *et al.* Detection of human brain cancer infiltration *ex vivo* and *in vivo* using quantitative optical coherence tomography. *Sci. Transl. Med.* **7,** 292ra100 (2015).
166. Ji, M. *et al.* Rapid, label-free detection of brain tumors with stimulated Raman scattering microscopy. *Sci. Transl. Med.* **5,** 201ra119 (2013).
167. Jermyn, M. *et al.* Intraoperative brain cancer detection with Raman spectroscopy in humans. *Sci. Transl. Med.* **7,** 274ra19 (2015).
168. Celli, J. P. *et al.* Imaging and photodynamic therapy: mechanisms, monitoring, and optimization. *Chem. Rev.* **110,** 2795–2838 (2010).
169. Yang, V. X. D., Muller, P. J., Herman, P. & Wilson, B. C. A multispectral fluorescence imaging system: design and initial clinical tests in intra-operative Photofrin-photodynamic therapy of brain tumors. *Lasers Surg. Med.* **32,** 224–232 (2003).
170. Ntziachristos, V. *et al.* Visualization of antitumor treatment by means of fluorescence molecular tomography with an annexin V-Cy5.5 conjugate. *Proc. Natl Acad. Sci. USA* **101,** 12294–12299 (2004).
171. Atreya, R. *et al. In vivo* imaging using fluorescent antibodies to tumor necrosis factor predicts therapeutic response in Crohn's disease. *Nat. Med.* **20,** 313–318 (2014).
172. Zhang, R. *et al.* Real-time *in vivo* Cherenkoscopy imaging during external beam radiation therapy. *J. Biomed. Opt.* **18,** 110504 (2013).
173. Grotjohann, T. *et al.* Diffraction-unlimited all-optical imaging and writing with a photochromic GFP. *Nature* **478,** 204–208 (2011).
174. Chen, B.-C. *et al.* Lattice light-sheet microscopy: imaging molecules to embryos at high spatiotemporal resolution. *Science* **346,** 1257998 (2014).
175. Yang, B. *et al.* Single-cell phenotyping within transparent intact tissue through whole-body clearing. *Cell* **158,** 945–958 (2014).
176. Mosk, A. P., Lagendijk, A., Lerosey, G. & Fink, M. Controlling waves in space and time for imaging and focusing in complex media. *Nat. Photon.* **6,** 283–292 (2012).
177. Doane, T. L. & Burda, C. The unique role of nanoparticles in nanomedicine: imaging, drug delivery and therapy. *Chem. Soc. Rev.* **41,** 2885–2911 (2012).
178. Youan, B. B. C. Chronopharmaceutical drug delivery systems: hurdles, hype or hope? *Adv. Drug Deliv. Rev.* **62,** 898–903 (2010).
179. Jayakumar, M. K. G., Idris, N. M. & Zhang, Y. Remote activation of biomolecules in deep tissues using near-infrared-to-UV upconversion nanotransducers. *Proc. Natl Acad. Sci. USA* **109,** 8483–8488 (2012).
180. Yavuz, M. S. *et al.* Gold nanocages covered by smart polymers for controlled release with near-infrared light. *Nat. Mater.* **8,** 935–939 (2009).
181. Carter, K. A. *et al.* Porphyrin-phospholipid liposomes permeabilized by near-infrared light. *Nat. Commun.* **5,** 3546 (2014).
182. Li, Y. *et al.* A smart and versatile theranostic nanomedicine platform based on nanoporphyrin. *Nat. Commun.* **5,** 4712 (2014).
183. Phillips, E. *et al.* Clinical translation of an ultrasmall inorganic optical-PET imaging nanoparticle probe. *Sci. Transl. Med.* **6,** 260ra149 (2014).
184. Kircher, M. F. *et al.* A brain tumor molecular imaging strategy using a new triple-modality MRI-photoacoustic-Raman nanoparticle. *Nat. Med.* **18,** 829–834 (2012).
185. Lin, J. *et al.* Photosensitizer-loaded gold vesicles with strong plasmonic coupling effect for imaging-guided photothermal/photodynamic therapy. *ACS Nano* **7,** 5320–5329 (2013).

186. Liu, J. *et al.* Bismuth sulfide nanorods as a precision nanomedicine for *in vivo* multimodal imaging-guided photothermal therapy of tumor. *ACS Nano* **9,** 696–707 (2015).
187. Spring, B. Q. *et al.* A photoactivable multi-inhibitor nanoliposome for tumour control and simultaneous inhibition of treatment escape pathways. *Nat. Nanotech.* **11,** 378–387 (2016).
188. Pasparakis, G., Manouras, T., Vamvakaki, M. & Argitis, P. Harnessing photochemical internalization with dual degradable nanoparticles for combinatorial photo-chemotherapy. *Nat. Commun.* **5,** 3623 (2014).
189. Lukianova-Hleb, E. Y. *et al.* On-demand intracellular amplification of chemoradiation with cancer-specific plasmonic nanobubbles. *Nat. Med.* **20,** 778–784 (2014).
190. Wilhelm, S. *et al.* Analysis of nanoparticle delivery to tumours. *Nat. Rev. Mater.* **1,** 16014 (2016).
191. Tong, R. & Langer, R. Nanomedicines targeting the tumor microenvironment. *Cancer J.* **21,** 314–321 (2015).
192. Douglas, S. M., Bachelet, I. & Church, G. M. A logic-gated nanorobot for targeted transport of molecular payloads. *Science* **335,** 831–834 (2012).
193. von Maltzahn, G. *et al.* Nanoparticles that communicate *in vivo* to amplify tumour targeting. *Nat. Mater.* **10,** 545–552 (2011).
194. Dai, B. *et al.* Programmable artificial phototactic microswimmer. *Nat. Nanotech.* http://dx.doi.org/10.1038/nnano.2016.187 (2016).
195. Boyden, E. S., Zhang, F., Bamberg, E., Nagel, G. & Deisseroth, K. Millisecond-timescale, genetically targeted optical control of neural activity. *Nat. Neurosci.* **8,** 1263–1268 (2005).
196. Gradinaru, V., Mogri, M., Thompson, K. R., Henderson, J. M. & Deisseroth, K. Optical deconstruction of parkinsonian neural circuitry. *Science* **324,** 354–359 (2009).
197. Creed, M., Pascoli, V. J. & Luscher, C. Refining deep brain stimulation to emulate optogenetic treatment of synaptic pathology. *Science* **347,** 659–664 (2015).
198. Williams, J. C. & Denison, T. From optogenetic technologies to neuromodulation therapies. *Sci. Transl. Med.* **5,** 177ps6 (2013).
199. Chow, B. Y. & Boyden, E. S. Optogenetics and translational medicine. *Sci. Transl. Med.* **5,** 177ps5 (2013).
200. Ramirez, S. *et al.* Activating positive memory engrams suppresses depression-like behaviour. *Nature* **522,** 335–339 (2015).
201. Iyer, S. M. *et al.* Virally mediated optogenetic excitation and inhibition of pain in freely moving nontransgenic mice. *Nat. Biotechnol.* **32,** 274–278 (2014).
202. Bruegmann, T. *et al.* Optogenetic control of contractile function in skeletal muscle. *Nat. Commun.* **6,** 7153 (2015).
203. Busskamp, V. & Roska, B. Optogenetic approaches to restoring visual function in retinitis pigmentosa. *Curr. Opin. Neurobiol.* **21,** 942–946 (2011).
204. Barrett, J. M., Berlinguer-Palmini, R. & Degenaar, P. Optogenetic approaches to retinal prosthesis. *Vis. Neurosci.* **31,** 345–354 (2014).
205. Kramer, R. H., Mourot, A. & Adesnik, H. Optogenetic pharmacology for control of native neuronal signaling proteins. *Nat. Neurosci.* **16,** 816–823 (2013).
206. Polosukhina, A. *et al.* Photochemical restoration of visual responses in blind mice. *Neuron* **75,** 271–282 (2012).
207. Mourot, A. *et al.* Rapid optical control of nociception with an ion-channel photoswitch. *Nat. Methods* **9,** 396–402 (2012).
208. Levitz, J. *et al.* Optical control of metabotropic glutamate receptors. *Nat. Neurosci.* **16,** 507–516 (2013).
209. Gaub, B. M. *et al.* Restoration of visual function by expression of a light-gated mammalian ion channel in retinal ganglion cells or ON-bipolar cells. *Proc. Natl Acad. Sci. USA* **111,** E5574–E5583 (2014).
210. Melyan, Z., Tarttelin, E. E., Bellingham, J., Lucas, R. J. & Hankins, M. W. Addition of human melanopsin renders mammalian cells photoresponsive. *Nature* **433,** 741–745 (2005).
211. Ye, H., Daoud-El Baba, M., Peng, R.-W. & Fussenegger, M. A synthetic optogenetic transcription device enhances blood-glucose homeostasis in mice. *Science* **332,** 1565–1568 (2011).
212. Choi, M. *et al.* Light-guiding hydrogels for cell-based sensing and optogenetic synthesis *in vivo*. *Nat. Photon.* **7,** 987–994 (2013).
213. Gao, L. *et al.* Epidermal photonic devices for quantitative imaging of temperature and thermal transport characteristics of the skin. *Nat. Commun.* **5,** 4938 (2014).
214. White, M. S. *et al.* Ultrathin, highly flexible and stretchable PLEDs. *Nat. Photon.* **7,** 811–816 (2013).
215. Wang, C. *et al.* User-interactive electronic skin for instantaneous pressure visualization. *Nat. Mater.* **12,** 899–904 (2013).
216. Lochner, C. M., Khan, Y., Pierre, A. & Arias, A. C. All-organic optoelectronic sensor for pulse oximetry. *Nat. Commun.* **5,** 5745 (2014).
217. Koh, A. *et al.* A soft, wearable microfluidic device for the capture, storage, and colorimetric sensing of sweat. *Sci. Transl. Med.* **8,** 366ra165 (2016).
218. Lee, H. *et al.* An endoscope with integrated transparent bioelectronics and theranostic nanoparticles for colon cancer treatment. *Nat. Commun.* **6,** 10059 (2015).
219. Mathieson, K. *et al.* Photovoltaic retinal prosthesis with high pixel density. *Nat. Photon.* **6,** 391–397 (2012).
220. Kim, R.-H. *et al.* Waterproof AlInGaP optoelectronics on stretchable substrates with applications in biomedicine and robotics. *Nat. Mater.* **9,** 929–937 (2010).
221. Kim, T. *et al.* Injectable, cellular-scale optoelectronics with applications for wireless optogenetics. *Science* **340,** 211–216 (2013).
222. Montgomery, K. L. *et al.* Wirelessly powered, fully internal optogenetics for brain, spinal and peripheral circuits in mice. *Nat. Methods* **12,** 969–974 (2015).
223. Park, S. I. *et al.* Soft, stretchable, fully implantable miniaturized optoelectronic systems for wireless optogenetics. *Nat. Biotechnol.* **33,** 1280–1286 (2015).
224. Jeong, J.-W. *et al.* Wireless optofluidic systems for programmable *in vivo* pharmacology and optogenetics. *Cell* **162,** 662–674 (2015).
225. Folcher, M. *et al.* Mind-controlled transgene expression by a wireless-powered optogenetic designer cell implant. *Nat. Commun.* **5,** 5392 (2014).
226. Ho, J. S. *et al.* Wireless power transfer to deep-tissue microimplants. *Proc. Natl Acad. Sci. USA* **111,** 7974–7979 (2014).
227. Lee, S. H., Jeong, C. K., Hwang, G.-T. & Lee, K. J. Self-powered flexible inorganic electronic system. *Nano Energy* **14,** 111–125 (2014).
228. Bae, B. *et al.* Polymeric photosensitizer-embedded self-expanding metal stent for repeatable endoscopic photodynamic therapy of cholangiocarcinoma. *Biomaterials* **35,** 8487–8495 (2014).
229. Choi, M., Humar, M., Kim, S. & Yun, S.-H. Step-index optical fiber made of biocompatible hydrogels. *Adv. Mater.* **27,** 4081–4086 (2015).
230. Nizamoglu, S. *et al.* Bioabsorbable polymer optical waveguides for deep-tissue photomedicine. *Nat. Commun.* **7,** 10374 (2015).
231. Canales, A. *et al.* Multifunctional fibers for simultaneous optical, electrical and chemical interrogation of neural circuits *in vivo*. *Nat. Biotechnol.* **33,** 277–284 (2015).
232. Humar, M. & Yun, S. H. Intracellular microlasers. *Nat. Photon.* **9,** 572–576 (2015).
233. Cho, S., Humar, M., Martino, N. & Yun, S. H. Laser particle stimulated emission microscopy. *Phys. Rev. Lett.* **117,** 193902 (2016).
234. van Allen, H. W. Some new applications of electricity and light in medicine. *N. Engl. J. Med.* **160,** 331–333 (1909).
235. Jacques, S. L. Optical properties of biological tissues: a review. *Phys. Med. Biol.* **58,** R37–R61 (2013).
236. Moritz, A. R. & Henriques, F. C. J. Studies of thermal injury: II. The relative importance of time and surface temperature in the causation of cutaneous burns. *Am. J. Pathol.* **23,** 695–720 (1947).
237. Srinivasan, R. Ablation of polymers and biological tissue by ultraviolet lasers. *Science* **234,** 559–565 (1986).
238. Cain, C. P. *et al.* ICNIRP guidelines: revision of guidelines on limits of exposure to laser radiation of wavelengths between 400 nm and 1.4 μm. *Health Phys.* **79,** 431–440 (2000).
239. Thekaekara, M. P. Solar radiation measurement: techniques and instrumentation. *Sol. Energy* **18,** 309–325 (1976).

Acknowledgements

This work was supported by the US National Institutes of Health Director's Pioneer Award (DP1-OD022296) and grants P41-EB015903, R01-EY025454 and R01-CA192878, and National Science Foundation grants ECCS-1505569 and CMMI-1562863.

Author contributions

S.H.Y. and S.J.J.K. conceived and wrote the manuscript.

Additional information

Reprints and permissions information is available at www.nature.com/reprints.

Correspondence should be addressed to S.H.Y.

How to cite this article: Yun, S. H. & Kwok, S. J. J. Light in diagnosis, therapy and surgery. *Nat. Biomed. Eng.* **1,** 0008 (2017).

Competing interests

The authors declare no competing financial interests.